PHYSICAL REVIEW D **87,** 114503 (2013)

Neutral B mixing in staggered chiral perturbation theory

C. Bernard

(The MILC Collaboration)

Department of Physics, Washington University, St. Louis, Missouri 63130, USA
(Received 15 March 2013; published 3 June 2013)

I calculate, at one loop in staggered chiral perturbation theory, the matrix elements of the complete set of five local operators that may contribute to B mixing both in the standard model and in beyond-the-standard-model theories. Lattice computations of these matrix elements by the Fermilab Lattice/MILC collaborations (and earlier by the HPQCD collaboration) convert a light staggered quark into a naive quark, and construct the relevant four-quark operators as local products of two local bilinears, each involving the naive light quark and the heavy quark. This particular representation of the operators turns out to be important in the chiral calculation, and it results in the presence of "wrong-spin" operators, whose contributions however vanish in the continuum limit. If the matrix elements of all five operators are computed on the lattice, then no additional low-energy constants are required to describe wrong-spin chiral effects.

DOI: 10.1103/PhysRevD.87.114503 PACS numbers: 12.38.Gc, 12.39.Fe, 13.20.He

I. INTRODUCTION

The mixing of neutral B mesons provides a fertile area for precision tests of the standard model. The fact that the mixing is a second order weak process and is also suppressed by small Cabibbo-Kobayashi-Maskawa angles in the standard model makes it sensitive to new physics. In order to take full advantage of experimental measurements of the mixing, one needs to determine the hadronic matrix elements of the effective weak operators. For B mixing the relevant operators are local four-quark operators with $\Delta b = 2$, where b is b-quark number, and the relevant states are B^0_d and $\bar{B}^0_d$ mesons or B^0_s and $\bar{B}^0_s$ mesons. A first-principle evaluation of such operator matrix elements is possible with lattice QCD.

Lattice computations usually involve an extrapolation in light quark masses to the physical up and down masses, and always require an extrapolation in lattice spacing a to $a = 0$, the continuum. These extrapolations can be controlled by using a version of chiral perturbation theory that includes the effects of the discretization errors associated with the choice of lattice action. In two recent lattice calculations of B mixing [1,2], staggered light quarks are combined with nonstaggered heavy quarks using nonrelativistic QCD [3] or the Fermilab action [4], respectively. In such cases, the appropriate chiral theory is "rooted, heavy-meson staggered chiral perturbation theory" (rHMSχPT) [5].

In this paper, I calculate B mixing to one-loop order in rHMSχPT. Roughly speaking, I work to leading order in the heavy-quark expansion, although I do include the large $1/m_B$ effects: the hyperfine splitting of B and B^* and the flavor splitting of B_s and B_d. This is a systematic approximation in the power counting introduced by Boyd and Grinstein [6] and discussed recently in Ref. [7] for the lattice calculation of heavy-light meson decay constants. If instead one prefers a power counting strictly in $1/m_B$, which sets the splittings to zero, it is easy to take that limit of the results given in this paper.

In the rHMSχPT calculation, it is important to take into account the exact form of the lattice operator used to approximate the continuum one. References [1,2] construct the four-quark operators as the local product of two local bilinears,[1] each formed from a heavy antiquark field and a light quark field with the "naive" lattice discretization. As proposed in Ref. [8] and discussed below, the naive field is constructed in turn from the simulated staggered fields (or more precisely, the naive propagator is constructed from the staggered propagator). Both the use of naive fields and the local nature of the four-quark operator influence the form of the corrections at one loop.

It is not hard to understand the qualitative effect of the lattice locality of the four-quark operator. Because of lattice doubling symmetry, a (single-component) staggered quark field actually corresponds to the 16 continuum degrees of freedom of four "tastes" of four-component Dirac particles. On the lattice, the spin and taste degrees of freedom can be made explicit in position space by combining the 16 staggered components associated with an elementary hypercube [9]. For our four-quark operators, the two light staggered quarks are tied to the same space-time point, so that their spin and tastes are coupled. The coupling produces undesired contributions to the operator, with "wrong spin" and "wrong taste." These undesired contributions appear at $\mathcal{O}(1)$ in the lattice spacing.

[1]That is, all four fields are located at the same lattice point.

 © 2013 American Physical Society

Fortunately, in the matrix elements considered here, continuum $SU(4)$ taste symmetry suppresses wrong-taste contributions and therefore wrong-spin contributions. On the lattice, $SU(4)$ taste symmetry is violated at $\mathcal{O}(a^2)$, so the undesired contributions come in at that order. Since $\mathcal{O}(a^2)$ corrections appear at one loop in rHMSχPT, that is the order at which we find wrong-spin, wrong-taste contributions to B mixing.

Similarly, it is clear that the effect of using naive quarks in the operators and interpolating fields must be to sum over tastes, since the naive quarks have no explicit taste index. However, the details are nontrivial. It turns out that the heavy-light meson propagator is simply an average over the initial and final tastes, which are equal to each other. The three-point function involves a complicated sum over tastes of the staggered quarks in the interpolating fields and four-quark operator, and there is coupling between the spin matrices in the operator and the taste sum. These details play a key part in the discussion below.

A calculation in rHMSχPT can be thought of as ''staggering'' the corresponding continuum calculation, which here would be in heavy-meson chiral perturbation theory. In fact, when the continuum calculation includes partial quenching effects, it is often possible to deduce the proper staggered version without having to recalculate explicitly any of the diagrams (see, for example, Ref. [10]). In the current case, a partially quenched continuum calculation does exist [11]. However, the complications due to the naive-to-staggered translation and the wrong spin-taste contributions make it necessary to perform the staggered calculation from scratch. Nevertheless, Ref. [11] is extremely useful here, and provides a check of the current results in the $a \to 0$ limit.

The B mixing matrix elements for any four-quark operator that can appear in the standard model and in possible extensions such as supersymmetry can be written in terms of the matrix elements of the following five operators [12]:

$$\begin{aligned} \mathcal{O}_1 &= (\bar{b}\gamma^\nu Lq)[\bar{b}\gamma^\nu Lq], \qquad \mathcal{O}_2 = (\bar{b}Lq)[\bar{b}Lq], \\ \mathcal{O}_3 &= (\bar{b}Lq][\bar{b}Lq), \qquad \mathcal{O}_4 = (\bar{b}Lq)[\bar{b}Rq], \\ \mathcal{O}_5 &= (\bar{b}Lq][\bar{b}Rq), \end{aligned} \tag{1}$$

where pairs of round or square parentheses indicate how the color indices are to be contracted, and R and L are the right and left projectors: $R = (1 + \gamma_5)/2$ and $L = (1 - \gamma_5)/2$. Operators, $\mathcal{O}_1$, $\mathcal{O}_2$ and $\mathcal{O}_3$ appear in the standard model, with $\mathcal{O}_1$ (which mixes with $\mathcal{O}_2$ under renormalization) governing the mass differences of the neutral B eigenstates, ΔM_d and ΔM_s. Operators $\mathcal{O}_4$ and $\mathcal{O}_5$ appear in extensions of the standard model. Additional operators with $R \leftrightarrow L$ can also contribute beyond the standard model, but parity implies that their mixing matrix elements in QCD are equal to those of the above operators. In addition to parity, Fierz transformations are needed in order to write the mixing matrix elements of any four-quark operator with these quantum numbers in terms of those in Eq. (1); for a detailed explanation see Ref. [13].

I note that the corresponding projectors R, L in Ref. [11] do not have the factor of $1/2$, so the operators there are differently normalized. Since in any case unknown low-energy constants will enter in the chiral theory, this normalization difference is unimportant here.

The fact that Eq. (1) is a complete set of operators for B mixing implies that wrong-spin contributions to the operators do not in fact lead to any new low-energy constants in the chiral theory. Wrong-spin contributions to operator $\mathcal{O}_i$ merely lead to the appearance of the low-energy constants associated with operators $\mathcal{O}_{j\neq i}$ in the one-loop expression for the $\mathcal{O}_i$ matrix element. Thus, a staggered lattice calculation that computes the matrix elements of all the operators in Eq. (1) will not suffer from increased systematic or statistical errors due to the wrong-spin issue. Existing calculations [1,2] study the matrix element of $\mathcal{O}_1$ exclusively. In the case of Ref. [1], the one-loop contributions of wrong-spin operators were not known at the time, so one presumably should include some additional systematic error in their result. In the case of Ref. [2], it was not possible to make a complete study of this effect because the matrix elements of the other operators were not computed. However, an associated systematic error was estimated.

In the relevant staggered simulations, the fourth root of the fermion determinant is taken in order to eliminate the fourfold multiplicity of tastes in the sea. The rooted theory then suffers from nonlocal violations of unitarity at nonzero lattice spacing [14,15]. However, there are strong theoretical arguments [16–19], as well as other analytical and numerical evidence [20–24], that the local, unitary theory of QCD is recovered in the continuum limit. Furthermore, it is straightforward to take rooting into account in the chiral theory. One simply needs to multiply each sea quark loop by a factor of $1/4$ [25,26]. This can be done either by following the quark flow [27] to locate the loops, or—more systematically—by replicating the sea quarks n_r times and taking $n_r = 1/4$ in the result of the chiral calculation [17,19]. Since I will need to work out the quark flows in any case, I use the former method below.

The remainder of this paper is organized as follows. Section II briefly reviews the basics of rHMSχPT, focusing in particular on those aspects that will be important here. In Sec. III, I discuss the connection between naive and staggered quarks, and how it influences the structure of the four-quark operators and the interpolating heavy-light meson fields. The calculation of the one-loop diagrams is detailed in Sec. IV. I also briefly explain why taste violations coming from mixing under renormalization do not need to be considered at this order. Section V compiles the final formulas for the chiral and continuum extrapolation of the matrix elements of the operators defined in Eq. (1); corresponding results for the B (''bag'') parameters are

collected in the Appendix. I conclude in Sec. VI and make some additional comments about existing and future lattice computations of B mixing. A preliminary account of the current calculation appears in Ref. [28].

Though I denote heavy quarks as b quarks and heavy mesons as B mesons throughout, the current calculation in rHMSχPT also applies to the local matrix elements in neutral D mixing, with the usual caveat that the omitted $1/m_Q$ terms (Q is a generic heavy quark) are larger in that case. However, long distance contributions are presumably much more important in the D case [29] than in the B case. Such contributions are beyond the scope of this work, and are likely to be difficult to compute on the lattice. See however Ref. [30] for a lattice approach to long-distance effects in the kaon system.

II. BASICS OF RHMSχPT

Here, I give a brief summary of some of the basic features and definitions from staggered chiral perturbation theory, both of heavy-light mesons and of light mesons ("pions"). In this summary, I follow Ref. [10] fairly closely, but adapt the notation slightly, to make it more similar to that of Ref. [11]. The reader is referred to the literature [5,10,25,26,31,32] for more details. For convenience in making connection to Ref. [11], I write the Lagrangian and do the perturbative calculations in Minkowski space.

Let $P_q^{(b)}$ be the field that annihilates the pseudoscalar meson containing a heavy quark b and a light quark $\bar{q}$ (the $\bar{B}_0$ for $q = d$), while $P_{\mu,q}^{*(b)}$ does the same for the vector meson ($\bar{B}_0^*$ for $q = d$). To take advantage of heavy-quark spin symmetry, pseudoscalar and vector fields are combined in the field

$$H_q^{(b)} = \frac{1+\not{v}}{2}[\gamma_{(M)}^{\mu} P_{\mu,q}^{*(b)} + i\gamma_5^{(M)} P_q^{(b)}], \tag{2}$$

which destroys a meson, while

$$\bar{H}_q^{(b)} = [\gamma_{(M)}^{\mu} P_{\mu,q}^{*(b)\dagger} + i\gamma_5^{(M)} P_q^{(b)\dagger}]\frac{1+\not{v}}{2} \tag{3}$$

creates a meson. Here v is the meson velocity, and the (M) on $\gamma_{(M)}^{\mu}$ and $\gamma_5^{(M)}$ indicates that they are Minkowski-space matrices: $\gamma_{(M)}^0 = \gamma^0$, $\gamma_{(M)}^j = i\gamma^j$, and $\gamma_5^{(M)} = \gamma_5$, with γ^{μ} and γ_5 the Euclidean (Hermitian) Dirac matrices. The label q indicates the "flavor-taste" index of the light quark in the meson. For n flavors of light quarks, q can take on $4n$ values. Later, I will write q as separate flavor (x) and taste (a) indices, $q \to (x, a)$.

Under $SU(2)$ heavy-quark spin symmetry, the heavy-light field transforms as

$$H^{(b)} \to S H^{(b)}, \qquad \bar{H}^{(b)} \to \bar{H}^{(b)} S^{\dagger}, \tag{4}$$

with $S \in SU(2)$, while under the $SU(4n)_L \times SU(4n)_R$ chiral symmetry,

$$H^{(b)} \to H^{(b)} \mathbb{U}^{\dagger}, \qquad \bar{H}^{(b)} \to \mathbb{U} \bar{H}^{(b)}, \tag{5}$$

with $\mathbb{U} \in SU(4n)$ defined below. We keep the light flavor and taste indices implicit here.

The light mesons are combined in a Hermitian field $\Phi(x)$. For n staggered flavors, Φ is a $4n \times 4n$ matrix given by

$$\Phi = \begin{pmatrix} U & \pi^+ & K^+ & \cdots \\ \pi^- & D & K^0 & \cdots \\ K^- & \overline{K^0} & S & \cdots \\ \vdots & \vdots & \vdots & \ddots \end{pmatrix}. \tag{6}$$

I show the $n = 3$ portion of Φ explicitly, and in fact detailed final results below will assume $n = 3$. Each entry in Eq. (A3) is a 4×4 matrix, written in terms of the 16 Hermitian basis elements of the Clifford taste algebra. It is convenient to take the generators of this algebra to be $\xi_{\mu} = \gamma_{\mu}^*$ [9], where $*$ denotes complex conjugation. Thus we write, for example,

$$U = \sum_{\Xi=1}^{16} U_{\Xi} \Gamma_{\Xi}^*, \tag{7}$$

$$\Gamma_{\Xi} = \{\gamma_5, i\gamma_{\mu}\gamma_5, \sigma_{\mu\nu}(\mu < \nu), \gamma_{\mu}, I\}, \tag{8}$$

with $\sigma_{\mu\nu} \equiv (i/2)[\gamma_{\mu}, \gamma_{\nu}]$.

It is useful to divide the indices Ξ into pairs of indices: $\Xi \to (\rho, t_{\rho})$, where ρ labels the SO(4) representation (P,A,T, V,I) and t_{ρ} labels the element within each representation. Thus t_{ρ} runs from 1 to N_{ρ}, where N_{ρ} is the dimension of each representation (1,4,6,4,1, respectively). We then can write

$$U = \sum_{\rho} \sum_{t_{\rho}=1}^{N_{\rho}} U_{\rho,t_{\rho}} \Gamma_{\rho,t_{\rho}}^*. \tag{9}$$

The component fields of the flavor-neutral elements of Φ (namely $U_{\rho,t_{\rho}}, D_{\rho,t_{\rho}}, \ldots$) are real; the other (flavor-charged) fields ($\pi_{\rho,t_{\rho}}^+, K_{\rho,t_{\rho}}^0, \ldots$) are complex.

The mass matrix is the $4n \times 4n$ matrix

$$\mathcal{M} = \begin{pmatrix} m_u I & 0 & 0 & \cdots \\ 0 & m_d I & 0 & \cdots \\ 0 & 0 & m_s I & \cdots \\ \vdots & \vdots & \vdots & \ddots \end{pmatrix}, \tag{10}$$

where the portion shown is again for the $n = 3$ case.

From Φ one constructs the unitary chiral field $\Sigma = \exp[i\Phi/f]$, with f the tree-level pion decay constant. In our normalization, $f \sim f_{\pi} \cong 131$ MeV. Terms involving the heavy-lights are conveniently written using $\sigma \equiv \sqrt{\Sigma} = \exp[i\Phi/2f]$. These fields transform trivially under the $SU(2)$ spin symmetry, while under $SU(4n)_L \times SU(4n)_R$ we have

$$\Sigma \to L \Sigma R^{\dagger}, \qquad \Sigma^{\dagger} \to R \Sigma^{\dagger} L^{\dagger}, \tag{11}$$

$$\sigma \to L\sigma\mathbb{U}^\dagger = \mathbb{U}\sigma R^\dagger, \quad \sigma^\dagger \to R\sigma^\dagger\mathbb{U}^\dagger = \mathbb{U}\sigma^\dagger L^\dagger, \tag{12}$$

with global transformations $L \in SU(4n)_L$ and $R \in SU(4n)_R$. The transformation $\mathbb{U}$, defined by Eq. (12), is a function of Φ and therefore of the coordinates.

It is convenient to define objects involving the σ field that transform only with $\mathbb{U}$ and $\mathbb{U}^\dagger$. The two possibilities with a single derivative are

$$\mathbb{V}_\mu = \frac{i}{2}[\sigma^\dagger\partial_\mu\sigma + \sigma\partial_\mu\sigma^\dagger], \tag{13}$$

$$\mathbb{A}_\mu = \frac{i}{2}[\sigma^\dagger\partial_\mu\sigma - \sigma\partial_\mu\sigma^\dagger]. \tag{14}$$

$\mathbb{V}_\mu$ transforms like a vector field under the $SU(4n)_L \times SU(4n)_R$ chiral symmetry and, when combined with the derivative, can form a covariant derivative acting on the heavy-light field or its conjugate:

$$\begin{aligned}(H^{(b)}\overleftarrow{D}_\mu)_q &= H^{(b)}_{q'}\overleftarrow{D}^{q'q}_\mu \equiv \partial_\mu H^{(b)}_q + iH^{(b)}_{q'}\mathbb{V}^{q'q}_\mu,\\ (\vec{D}_\mu\bar{H}^{(b)})_q &= \vec{D}^{qq'}_\mu\bar{H}^{(b)}_{q'} \equiv \partial_\mu\bar{H}^{(b)}_q - i\mathbb{V}^{qq'}_\mu\bar{H}^{(b)}_{q'},\end{aligned} \tag{15}$$

with implicit sums over repeated indices. The covariant derivatives and $\mathbb{A}_\mu$ transform under the chiral symmetry as

$$\begin{aligned}H^{(b)}\overleftarrow{D}_\mu \to (H^{(b)}\overleftarrow{D}_\mu)\mathbb{U}^\dagger, \qquad \vec{D}_\mu\bar{H}^{(b)} \to \mathbb{U}(\vec{D}_\mu\bar{H}^{(b)}),\\ \mathbb{A}_\mu \to \mathbb{U}\mathbb{A}_\mu\mathbb{U}^\dagger.\end{aligned} \tag{16}$$

We can write the leading order (LO) chiral Lagrangian as

$$\mathcal{L}_{\rm LO} = \mathcal{L}_{\rm pion} + \mathcal{L}_{\rm HL}, \tag{17}$$

where $\mathcal{L}_{\rm pion}$ is the standard staggered chiral perturbation theory (SχPT) Lagrangian for the light-light mesons, and $\mathcal{L}_{\rm HL}$ is the contribution of the heavy-lights. In Minkowski space, we have

$$\begin{aligned}\mathcal{L}_{\rm pion} = \frac{f^2}{8}\,{\rm Tr}(\partial_\mu\Sigma\partial^\mu\Sigma^\dagger) + \frac{1}{4}\mu f^2\,{\rm Tr}(\mathcal{M}\Sigma + \mathcal{M}\Sigma^\dagger)\\ - \frac{2m_0^2}{3}(U_I + D_I + S_I + \cdots)^2 - a^2\mathcal{V},\end{aligned} \tag{18}$$

$$\begin{aligned}-\mathcal{V} = {}& C_1\,{\rm Tr}(\xi_5\Sigma\xi_5\Sigma^\dagger) + C_3\frac{1}{2}\sum_\nu[{\rm Tr}(\xi_\nu\Sigma\xi_\nu\Sigma) + {\rm H.c.}] + C_4\frac{1}{2}\sum_\nu[{\rm Tr}(i\xi_\nu\xi_5\Sigma i\xi_\nu\xi_5\Sigma) + {\rm H.c.}]\\ &+ C_6\sum_{\mu<\nu}{\rm Tr}(\xi_{\mu\nu}\Sigma\xi_{\mu\nu}\Sigma^\dagger) + C_{2V}\frac{1}{4}\sum_\nu[{\rm Tr}(\xi_\nu\Sigma)\,{\rm Tr}(\xi_\nu\Sigma) + {\rm H.c.}] + C_{2A}\frac{1}{4}\sum_\nu[{\rm Tr}(i\xi_\nu\xi_5\Sigma)\,{\rm Tr}(i\xi_\nu\xi_5\Sigma) + {\rm H.c.}]\\ &+ C_{5V}\frac{1}{2}\sum_\nu{\rm Tr}(\xi_\nu\Sigma)\,{\rm Tr}(\xi_\nu\Sigma^\dagger) + C_{5A}\frac{1}{2}\sum_\nu{\rm Tr}(i\xi_\nu\xi_5\Sigma)\,{\rm Tr}(i\xi_\nu\xi_5\Sigma^\dagger),\end{aligned} \tag{19}$$

$$\mathcal{L}_{\rm HL} = -i\,{\rm Tr}(\bar{H}^{(b)}H^{(b)}v\cdot\overleftarrow{D}) + g_\pi\,{\rm Tr}(\bar{H}^{(b)}H^{(b)}\gamma^\mu_{(M)}\gamma^{(M)}_5\mathbb{A}_\mu). \tag{20}$$

Here Tr denotes a trace over flavor-taste indices and, where relevant, Dirac indices. The product $\bar{H}^{(b)}H^{(b)}$ is treated as a matrix in flavor-taste space: $(\bar{H}^{(b)}H^{(b)})_{qq'} \equiv \bar{H}^{(b)}_q H^{(b)}_{q'}$. The covariant derivative $\overleftarrow{D}$ acts only on the field immediately preceding it. For convenience, I work with diagonal fields $(U, D, \ldots)$ and leave the anomaly (m_0^2) term explicit in Eq. (18). We can take $m_0^2 \to \infty$ and go to the physical basis $(\pi^0, \eta, \ldots)$ at the end of the calculation [33].

At tree level, the light-light meson composed of quarks of flavor x and y, and with $SO(4)$ taste representation ρ, is

$$M^2_{xy,\rho} = \mu(m_x + m_y) + a^2\Delta_\rho. \tag{21}$$

Here Δ_ρ is the taste splitting, which can be expressed in terms of C_1, C_3, C_4 and C_6 in Eq. (19) [25]. The residual $SO(4)$ taste symmetry [31] at this order implies that the mesons within a given taste representation are degenerate in mass.

I now list some key expressions from the Feynman rules given in Ref. [10], but adapted to the current notation. Using separate indices for flavor (x, y) and taste (a, a', c, c'), the (quark-line) connected pion propagator in Minkowski space is

$$\{\Phi^{xy}_{aa'}\Phi^{yx}_{c'c}\}_{\rm conn}(p) = \sum_\rho\frac{i}{p^2 - M^2_{xy,\rho} + i\epsilon}\Big[\sum_{t_\rho}\Gamma^{\rho,t_\rho}_{a'a}\Gamma^{\rho,t_\rho}_{cc'}\Big]. \tag{22}$$

Here, I have used the fact that Γ^{ρ,t_ρ} is Hermitian to replace the complex conjugation in Eq. (9) by interchange of indices on the right-hand side, which will be convenient later.

Similarly, the disconnected (hairpin) propagator is

$$\{\Phi^{xx}_{aa'}\Phi^{yy}_{c'c}\}_{\rm disc}(p) \equiv \sum_\rho\mathcal{D}^\rho_{xx,yy}\Big[\sum_{t_\rho}\Gamma^{\rho,t_\rho}_{a'a}\Gamma^{\rho,t_\rho}_{cc'}\Big], \tag{23}$$

where

$$\mathcal{D}^{\rho}_{xx,yy} = -i\delta'_{\rho}\frac{i}{(p^2 - M^2_{X,\rho} + i\epsilon)}\frac{i}{(p^2 - M^2_{Y,\rho} + i\epsilon)} \times \frac{(p^2 - M^2_{U,\rho})(p^2 - M^2_{S,\rho})}{(p^2 - M^2_{\eta,\rho} + i\epsilon)(p^2 - M^2_{\eta',\rho} + i\epsilon)}, \quad (24)$$

with the hairpin strength δ'_ρ given by

$$\delta'_\rho = \begin{cases} a^2\delta'_V, & \rho = V \text{ (taste vector)}; \\ a^2\delta'_A, & \rho = A \text{ (taste axial vector)}; \\ 4m_0^2/3, & \rho = I \text{ (taste singlet)}; \\ 0, & \rho = T, P \text{ (taste tensor or pseudoscalar)}. \end{cases} \quad (25)$$

X and Y denote valence mesons made from $x\bar{x}$ or $y\bar{y}$ quarks, respectively, with M_X and M_Y their masses. For the sea mesons, the masses M_U and M_S do not include the mixing effects of the hairpins. The rediagonalized states after including the hairpins are η and η'. For concreteness I have assumed the 2 + 1 case: $m_u = m_d$.

The propagators for the heavy-light mesons are

$$\{P^{(b)}_{xa}P^{(b)\dagger}_{yc}\}(k) = \frac{i\delta_{ac}\delta_{xy}}{2(v\cdot k + i\epsilon)}, \quad (26)$$

$$\{P^{*(b)}_{\mu xa}P^{*(b)\dagger}_{\nu yc}\}(k) = \frac{-i\delta_{ac}\delta_{xy}(g_{\mu\nu} - v_\mu v_\nu)}{2(v\cdot k - \Delta^* + i\epsilon)}, \quad (27)$$

where Δ^* is the B^*-B mass splitting. The $\bar{B}\bar{B}^*\pi$ vertex (including the i from $\exp(i\mathcal{L})$) is

$$\frac{g_\pi}{f}(P^{(b)\dagger}_{xa}P^{*(b)}_{\mu yc} - P^{*(b)\dagger}_{\mu xa}P^{(b)}_{yc})\partial^\mu\Phi^{yx}_{ca}, \quad (28)$$

where the repeated indices a, x, y, c, and μ are summed.

For B mixing, we also need corresponding fields that destroy and create mesons with $\bar{b}$ quarks, i.e., B_0-like and B_0^*-like mesons. These fields and their interactions can be obtained from the previous ones using charge conjugation [34]. The individual meson fields are indicated by, for example, $P^{*(\bar{b})}_{\mu,q}$ and $P^{(\bar{b})}_q$. (Note that the light quark label q does not distinguish between quarks and antiquarks.) The combined fields are

$$H^{(\bar{b})}_q = [\gamma^\mu_{(M)}P^{*(\bar{b})}_{\mu,q} + i\gamma^{(M)}_5 P^{(\bar{b})}_q]\frac{1 - \not{v}}{2}, \quad (29)$$

$$\bar{H}^{(\bar{b})}_q = \frac{1 - \not{v}}{2}[\gamma^\mu_{(M)}P^{*(\bar{b})\dagger}_{\mu,q} + i\gamma^{(M)}_5 P^{(\bar{b})\dagger}_q]. \quad (30)$$

The propagators for the $P^{*(\bar{b})}_{\mu,q}$ and $P^{(\bar{b})}_q$ fields are the same as those for the $P^{*(b)}_{\mu,q}$ and $P^{(b)}_q$ fields, Eqs. (26) and (27). The $BB^*\pi$ vertex is

$$\frac{g_\pi}{f}(P^{(\bar{b})}_{xa}P^{*(\bar{b})\dagger}_{\mu yc} - P^{*(\bar{b})}_{\mu xa}P^{(\bar{b})\dagger}_{yc})\partial^\mu\Phi^{yx}_{ca}. \quad (31)$$

III. TRANSLATING FROM NAIVE TO STAGGERED QUARKS

The naive light quark action may be rewritten as four copies of the staggered action:

$$\Psi(x) = \Omega(x)\underline{\chi}(x); \qquad \Omega(x) = \gamma_0^{x_0}\gamma_1^{x_1}\gamma_2^{x_2}\gamma_3^{x_3}, \quad (32)$$

where $\Psi(x)$ is the naive quark field and $\underline{\chi}(x)$ is a "copied" staggered field, with each Dirac component $\underline{\chi}_i$ separately having the staggered action. I call "copy symmetry" the $SU(4)$ that acts on the copy index i. Unlike the $SU(4)$ vector taste symmetry, which acts on individual staggered fields (written in the spin-taste basis) and is exact for an interacting theory only in the continuum limit, copy symmetry is an exact lattice symmetry. Thus the propagator of a copied staggered field is

$$\langle\underline{\chi}_i(x)\bar{\underline{\chi}}_{i'}(y)\rangle = \delta_{i,i'}\langle\chi(x)\bar{\chi}(y)\rangle, \quad (33)$$

where χ is the normal (uncopied) staggered field. This implies

$$\langle\Psi(x)\bar{\Psi}(y)\rangle = \Omega(x)\Omega^\dagger(y)\langle\chi(x)\bar{\chi}(y)\rangle. \quad (34)$$

In the simulations using staggered quarks, the naive field is never constructed *per se*; instead Eq. (34) is used to translate staggered propagators into naive propagators [8].

An interpolating field $\mathcal{H}(x)$ for a B_q meson is

$$\mathcal{H}(x) = \bar{b}(x)\gamma_5\Psi(x) = \bar{b}(x)\gamma_5\Omega(x)\underline{\chi}(x). \quad (35)$$

I assume that in practical applications $\mathcal{H}(x)$ will always be summed over a time slice, either explicitly, or implicitly by using translation invariance.

To leading order in a, $b(x)$ varies smoothly (up to gauge transformation) between neighboring spatial sites, but $\underline{\chi}$ does not, due to taste doubling. On the other hand, in the spin-taste basis, which we arrive at by summing the staggered fields over hypercubes, the staggered fields are smooth on the doubled lattice. We are thus led to focus on the average of $\mathcal{H}(x)$ over a spatial cube. Let $x = (t, \boldsymbol{x})$ with $\boldsymbol{x} = 2\boldsymbol{y}$ even, and let $\eta = (\eta_0, \boldsymbol{\eta})$ be a 4-vector with all components 0 or 1. For t even ($t = 2\tau$) the averaged field is

$$\begin{aligned}\mathcal{H}^{(\mathrm{av})}(t,\boldsymbol{x}) &= \frac{1}{8}\sum_{\boldsymbol{\eta}}\bar{b}(t,\boldsymbol{x}+\boldsymbol{\eta})\gamma_5\Omega(2\tau,\boldsymbol{\eta})\underline{\chi}(2\tau,2\boldsymbol{y}+\boldsymbol{\eta}) \\ &\cong \frac{1}{8}\bar{b}(t,\boldsymbol{x})\gamma_5\sum_{\boldsymbol{\eta}}\Omega(\boldsymbol{\eta})\underline{\chi}(2\tau,2\boldsymbol{y}+\boldsymbol{\eta}) \\ &\cong \frac{1}{16}\bar{b}(t,\boldsymbol{x})\gamma_5\sum_{\eta}[\Omega(\eta)\underline{\chi}(2\tau+\eta_0,2\boldsymbol{y}+\boldsymbol{\eta}) \\ &\quad + (-1)^{\eta_0}\Omega(\eta)\underline{\chi}(2\tau+\eta_0,2\boldsymbol{y}+\boldsymbol{\eta})]. \quad (36)\end{aligned}$$

Inserted gauge links for gauge invariance of point-split quantities are implicit. For t odd ($t = 2\tau + 1$), the result is the same except the term on the last line of Eq. (36)

changes sign. Using the fact that $(-1)^{\eta_0}\Omega(\eta) = \gamma_5\gamma_0\Omega(\eta)\gamma_0\gamma_5$, it is not hard to see that this second term just gives the usual staggered oscillating (in time) state with opposite parity. I have dropped higher order terms in a coming from the variation of the heavy-quark field over the cube. For simplicity, we simply assume from now on that all components of x are even ($x_\mu = 2y_\mu$), and that the oscillating state has been removed by the fitting procedure. We then have

$$\mathcal{H}^{(\mathrm{av})}(x) \to \frac{1}{16}\bar{b}(x)\gamma_5\sum_\eta \Omega(\eta)\underline{\chi}(2y+\eta). \tag{37}$$

We now convert to a spin-taste basis for the staggered fields. The standard construction for a single staggered field is [9]

$$q^{\alpha a}(y) = \frac{1}{8}\sum_\eta \Omega^{\alpha a}(\eta)\chi(2y+\eta), \tag{38}$$

where α is a spin index and a is a taste index. As is well known [35–37], this decomposition is correct only to lowest order in a and generates a spurious $\mathcal{O}(a)$ term in the spin-taste action, but it is good enough for our purposes. Here we need a copied version:

$$q_i^{\alpha a}(y) = \frac{1}{8}\sum_\eta \Omega^{\alpha a}(\eta)\underline{\chi}_i(2y+\eta). \tag{39}$$

With spin indices implicit, Eq. (37) then becomes

$$\mathcal{H}^{(\mathrm{av})}(x) \to \frac{1}{2}\bar{b}(x)\gamma_5 q_i^a(y)\delta_i^a, \tag{40}$$

where repeated indices are summed. With Eq. (33), this implies that the contraction of $\mathcal{H}$ with $\mathcal{H}^\dagger$ (i.e., the heavy-light propagator) is automatically averaged over tastes:

$$\langle \mathcal{H}(x)\mathcal{H}^\dagger(x')\rangle \sim \frac{1}{4}\langle \bar{b}(x)\gamma_5 q^a(y)\bar{q}^a(y')\gamma_5 b(x')\rangle, \tag{41}$$

where a sum over a is implicit.

Analysis of the four-quark operator is more complicated because the two bilinears from which it is constructed are not separately summed over space; only the four-quark operator is summed. However, we can write it in terms of separately summed bilinears by using the identities

$$\frac{1}{256}\sum_K \mathrm{tr}(\Omega(\eta)K\Omega^\dagger(\eta)K)\,\mathrm{tr}(\Omega(\eta')K\Omega^\dagger(\eta')K) = \delta_{\eta,\eta'}, \tag{42}$$

$$\frac{1}{4}\,\mathrm{tr}(\Omega(\eta)K\Omega^\dagger(\eta)K)\Omega(\eta) = K\Omega(\eta)K. \tag{43}$$

Here K is any of the 16 independent Hermitian matrices Γ_Ξ in Eq. (8), which obey $K^2 = I$. We get, for operator $\mathcal{O}_n = \bar{b}\Gamma_n\Psi\bar{b}\Gamma'_n\Psi$:

$$\begin{aligned}\mathcal{O}_n^{(\mathrm{av})}(x) &= \frac{1}{8}\sum_{\boldsymbol{\eta}} \bar{b}(t,2y+\eta)\Gamma_n\Psi(t,2y+\eta)\\ &\quad\times \bar{b}(t,2y+\eta)\Gamma'_n\Psi(t,2y+\eta)\\ &\to \frac{1}{4}\sum_K (\bar{b}\Gamma_n K q_k^c \bar{b}\Gamma'_n K q_\ell^d)K_{ck}K_{d\ell}.\end{aligned} \tag{44}$$

Here we have dropped the "wrong parity" part, which does not contribute if oscillating terms are removed by the fitting procedure. Note that contributions with $K \neq I$ have incorrect spin ($\Gamma_n K \otimes \Gamma'_n K$ instead of $\Gamma_n \otimes \Gamma'_n$), and coupling of taste (c, d) and copy (k, ℓ) indices.

There are $\mathcal{O}(a)$ and higher corrections to Eqs. (40) and (44), coming from the variations of the heavy quark field over the spatial cube and from corrections to the spin-taste construction in position space. As discussed in Sec. IV C, however, such terms do not contribute to nonanalytic terms in chiral perturbation theory until next-to-next-to-leading order (NNLO).

Using Eqs. (40) and (44), copy symmetry [Eq. (33)] implies

$$\langle \mathcal{H}^{(\mathrm{av})\dagger}\mathcal{O}_n^{(\mathrm{av})}\mathcal{H}^{(\mathrm{av})\dagger}\rangle \propto \langle D^{ca}D^{de}\rangle K_{ca}K_{de}, \tag{45}$$

where D^{ca} is the quark propagator (in a given background) for taste a into taste c. If taste symmetry is exact, $\langle D^{ca}D^{de}\rangle \propto \delta_{ac}\delta_{ed}$, and only the correct spin ($K = I$) contributes. Thus the desired matrix element will be obtained in the continuum limit.

At one loop, however, taste violations allow $\langle D^{ac}D^{ed}\rangle$ not to be proportional to $\delta_{ac}\delta_{ed}$, and terms with incorrect spins can contribute. For example, the taste-violating hairpin with vector taste can give a term proportional to $\xi^\mu_{ca}\xi^\mu_{de} = \gamma^\mu_{ac}\gamma^\mu_{ed}$. Then, since $\mathrm{tr}(\gamma^\mu K) = 4\delta_{K,\gamma_\mu}$, the spin of the operator is $\Gamma_n\gamma_\mu \otimes \Gamma'_n\gamma_\mu$ instead of $\Gamma_n \otimes \Gamma'_n$.

Equation (44) may be simplified by taking advantage of the exact $SO(4)$ taste symmetry of the staggered chiral theory at one loop. Within any $SO(4)$ multiplet $\kappa \in \{P, A, T, V, I\}$ with dimension $N_\kappa > 1$ (e.g., the vector-taste multiplet V with $N_V = 4$), the value of all one-loop diagrams would be unchanged if we replaced any multiplet element in the taste factors $K_{ck}K_{d\ell}$ with another element from the same multiplet.[2] We therefore write $K = \Gamma^{\kappa,t_\kappa}$, where t_κ labels the element within multiplet κ. Replacing the sum over K in Eq. (44) with a double sum over κ, t_κ, and using the $SO(4)$ symmetry, we then have

$$\mathcal{O}_n^{(\mathrm{av})}(x) \to \frac{1}{4}\sum_{\kappa,t'_\kappa}(\bar{b}\Gamma_n\Gamma^{\kappa,t'_\kappa}q_k^c\bar{b}\Gamma'_n\Gamma^{\kappa,t'_\kappa}q_\ell^d)\frac{1}{N_\kappa}\sum_{t_\kappa}\Gamma^{\kappa,t_\kappa}_{ck}\Gamma^{\kappa,t_\kappa}_{d\ell}. \tag{46}$$

Within a given multiplet, this decouples the sum over spins from the sum over tastes.

[2]Although indices k and ℓ are copy, not taste, indices at this point, they will become taste indices *à la* Eq. (45) shortly.

Thus, for a given continuum operator $\mathcal{O}_n$, the plan is to calculate the one-loop diagrams for each of the operators

$$\mathcal{O}_n^\kappa \equiv \sum_{t'_\kappa} \bar{b}\,\Gamma_n \Gamma^{\kappa,t'_\kappa} q_k^c \bar{b} \Gamma'_n \Gamma^{\kappa,t'_\kappa} q_\ell^d \tag{47}$$

between external (interpolating) fields $(\mathcal{H}^\dagger)_i^a$ and $(\mathcal{H}^\dagger)_j^e$, where, from Eq. (40),

$$(\mathcal{H}^\dagger)_i^a \equiv \bar{q}_i^a \gamma_5 b. \tag{48}$$

Each diagram for operator $\mathcal{O}_n^\kappa$ then gets an additional factor $\tilde{F}_\kappa$ coming from Eqs. (46) and (40), where

$$\tilde{F}_\kappa \equiv \frac{1}{16 N_\kappa} \sum_{t'_\kappa} \Gamma_{ck}^{\kappa,t'_\kappa} \Gamma_{d\ell}^{\kappa,t'_\kappa} \delta_{ai} \delta_{ej}. \tag{49}$$

Whether explicitly indicated or not, all repeated indices will then be summed; this includes taste and copy indices (a, c, d, e and i, j, k, ℓ) as well as the indices with dual, spin-taste meaning (κ, t_κ, t'_κ).

IV. CALCULATION OF ONE-LOOP DIAGRAMS FOR O_n

A. Procedure

We now set up one-loop rHMSχPT for the operators described above. We follow Ref. [11] as much as possible, but must take into account the complications of copy and taste indices. It is convenient first to express the operators $\mathcal{O}_n^\kappa$, given in Eq. (47) in terms of the basis of Eq. (1). From the relations among operators listed for example in Ref. [13] we find

$$\begin{aligned} &\mathcal{O}_1^P = \mathcal{O}_1, \quad \mathcal{O}_1^A = -8\mathcal{O}_2 - 8\mathcal{O}_3, \quad \mathcal{O}_1^T = -6\mathcal{O}_1, \\ &\mathcal{O}_1^V = 8\mathcal{O}_2 + 8\mathcal{O}_3, \quad \mathcal{O}_1^I = \mathcal{O}_1, \end{aligned} \tag{50}$$

$$\begin{aligned} &\mathcal{O}_2^P = \mathcal{O}_2, \quad \mathcal{O}_2^A = -\mathcal{O}_1, \quad \mathcal{O}_2^T = -2\mathcal{O}_2 - 4\mathcal{O}_3, \\ &\mathcal{O}_2^V = \mathcal{O}_1, \quad \mathcal{O}_2^I = \mathcal{O}_2, \end{aligned} \tag{51}$$

$$\begin{aligned} &\mathcal{O}_3^P = \mathcal{O}_3, \quad \mathcal{O}_3^A = -\mathcal{O}_1, \quad \mathcal{O}_3^T = -4\mathcal{O}_2 - 2\mathcal{O}_3, \\ &\mathcal{O}_3^V = \mathcal{O}_1, \quad \mathcal{O}_3^I = \mathcal{O}_3, \end{aligned} \tag{52}$$

$$\begin{aligned} &\mathcal{O}_4^P = -\mathcal{O}_4, \quad \mathcal{O}_4^A = -2\mathcal{O}_5, \quad \mathcal{O}_4^T = 0, \\ &\mathcal{O}_4^V = -2\mathcal{O}_5, \quad \mathcal{O}_4^I = \mathcal{O}_4, \end{aligned} \tag{53}$$

$$\begin{aligned} &\mathcal{O}_5^P = -\mathcal{O}_5, \quad \mathcal{O}_5^A = -2\mathcal{O}_4, \quad \mathcal{O}_5^T = 0, \\ &\mathcal{O}_5^V = -2\mathcal{O}_4, \quad \mathcal{O}_5^I = \mathcal{O}_5. \end{aligned} \tag{54}$$

The chiral representatives of the standard operators on the right-hand side of Eqs. (50) through (54) are given in Ref. [11]. There, the only relevant quantum number of the light quarks is their flavor, and both bilinears have the same flavor, which is labeled q. Here we also need to label the taste and, for the moment, the copy index of the light quarks, and these are not in general the same for both light quarks in the operator. So we adopt the notation $q \to x$, c, k, where x labels the quark flavor only, c (or other letters near the beginning of the alphabet) labels the quark taste, and k (or other letters near the middle of the alphabet) labels the quark copy. From [11], we then have

$$\begin{aligned} O_1^{xck;xd\ell} &= \beta_1[(\sigma P^{(b)\dagger})_{x,c,k}(\sigma P^{(\bar{b})})_{x,d,\ell} \\ &\quad + (\sigma P_\mu^{*(b)\dagger})_{x,c,k}(\sigma P^{*(\bar{b}),\mu})_{x,d,\ell}], \\ O_{2(3)}^{xck;xd\ell} &= \beta_{2(3)}(\sigma P^{(b)\dagger})_{x,c,k}(\sigma P^{(\bar{b})})_{x,d,\ell} \\ &\quad + \beta'_{2(3)}(\sigma P_\mu^{*(b)\dagger})_{x,c,k}(\sigma P^{*(\bar{b}),\mu})_{x,d,\ell}, \\ O_{4(5)}^{xck;xd\ell} &= \frac{\beta_{4(5)}}{2}[(\sigma P^{(b)\dagger})_{x,c,k}(\sigma^\dagger P^{(\bar{b})})_{x,d,\ell} \\ &\quad + (\sigma^\dagger P^{(b)\dagger})_{x,c,k}(\sigma P^{(\bar{b})})_{x,d,\ell}] \\ &\quad + \frac{\beta'_{4(5)}}{2}[(\sigma P_\mu^{*(b)\dagger})_{x,c,k}(\sigma^\dagger P^{*(\bar{b}),\mu})_{x,d,\ell} \\ &\quad + (\sigma^\dagger P_\mu^{*(b)\dagger})_{x,c,k}(\sigma P^{*(\bar{b}),\mu})_{x,d,\ell}]. \end{aligned} \tag{55}$$

The method used to obtain these operators in Ref. [11] is a standard spurion analysis. The factors of σ and $\sigma^\dagger$ are present in order make the light-quark spurions, which transform by left or right chiral rotations in Eq. (1), into objects that transform with $\mathbb{U}$ [defined in Eq. (12)] and can combine with the heavy-meson fields $\bar{H}_q^{(b)}$ and $H_q^{(\bar{b})}$ to make invariants. Although many insertions of Dirac matrices are possible in forming the invariants, they all reduce down to the simple forms in Eq. (55) when expressed in terms of $P^{(b)\dagger}$, $P^{(\bar{b})}$, $P_\mu^{*(b)\dagger}$, and $P_\mu^{*(\bar{b})}$. As pointed out in Ref. [34], this follows from heavy-quark spin symmetry, which relates the amplitude for B–$\bar{B}$ mixing to that of B^*–$\bar{B}^*$.

In Eq. (55), I have used the fact that we are only interested in the parity-even part of these operators to set the two coefficients Detmold and Lin call $\beta_{4(5)}$ and $\hat{\beta}_{4(5)}$ simply to $\beta_{4(5)}/2$. So where they have $\beta_{4(5)} + \hat{\beta}_{4(5)}$ we will have simply $\beta_{4(5)}$, and similarly for $\beta'_{4(5)}$ and $\hat{\beta}'_{4(5)}$. We use the Latin O for the chiral operators to distinguish them from quark-level operators $\mathcal{O}$. The external interpolating $\bar{B}$ and B fields are taken to be, respectively,

$$P_{x,a,i}^{(b)} \quad \text{and} \quad P_{x,e,j}^{(\bar{b})\dagger}. \tag{56}$$

Strictly speaking, there should be a second set of terms on the right-hand sides in Eq. (55) in which the pairs of indices c, k and d, ℓ are interchanged. These come about because the light quark field in either of the bilinears of the operator can be the one that creates the light antiquark in the $\bar{B}$ or annihilates the light quark in the B. However, since Eq. (49) is symmetric under this interchange, the extra terms give identical results to the ones we have

already, and therefore can be dropped at this point. Note that the β_i are low-energy constants with arbitrary normalization.

We can now use copy symmetry to simplify the equations, and ultimately eliminate the copy indices entirely. However, this cannot be done without taking into account the quark flow through the diagrams: copy symmetry works at the level of the light quark propagators, and not on meson propagators *per se*. The point is that a given light quark in an external meson field can end up in either a (b)- or $(\bar{b})$-labeled meson field in Eq. (55), and the copy symmetry has a different effect on the diagram in the two cases. If the light quark in the external $P^{(b)}_{x,a,i}$ field contracts with the quark in a (b)-labeled meson field (which has taste and copy indices c, k), then the combination of copy symmetry (which gives δ_{ik}) and the δ_{ai} in Eq. (49) forces $k = a$. On the other hand, if the same light quark contracts with the quark in a $(\bar{b})$-labeled meson field (indices d, ℓ), then we have $\ell = a$. So $\tilde{F}_\kappa$ will end up with a different taste structure in the two cases. For convenience, I prefer to rename the taste indices ($c \leftrightarrow d$) in the second case so that $\tilde{F}_\kappa$ remains the same. In doing so I adopt the convention that the taste-a quark in the external (b)-labeled field always contracts with the taste-c quark in the operator, but that taste-c quark may be in either the (b)- or the $(\bar{b})$-labeled meson field of the operator. Similarly, the taste-e quark in the external $(\bar{b})$ field always contracts with the taste-d quark in the operator.

Keeping the above points in mind, we now eliminate the copy indices completely from the calculation. With the exception of the wave-function renormalization diagrams, which of course do not involve the four-quark operators at all, the final procedure is as follows:

(1) For a particular operator $\mathcal{O}_n$ of interest, we first write the related operators $\mathcal{O}^\kappa_n$ as linear combinations of the standard operators, following Eqs. (50) through (54). It will be convenient then to define $\beta^{(\kappa)}_n$ and $\beta^{\prime(\kappa)}_n$ as the β and β' corresponding to operator $\mathcal{O}^\kappa_n$. Table I for $\beta^{(\kappa)}_n$ follows immediately from Eqs. (50) through (54).

TABLE I. Values of $\beta^{(\kappa)}_n$. For $\beta^{\prime(\kappa)}_n$, simply put primes on all entries in the table, with the understanding that $\beta'_1 = \beta_1$ [see Eq. (55)].

			κ		
n	P	A	T	V	I
1	β_1	$-8\beta_2 - 8\beta_3$	$-6\beta_1$	$8\beta_2 + 8\beta_3$	β_1
2	β_2	$-\beta_1$	$-2\beta_2 - 4\beta_3$	β_1	β_2
3	β_3	$-\beta_1$	$-4\beta_2 - 2\beta_3$	β_1	β_3
4	$-\beta_4$	$-2\beta_5$	0	$-2\beta_5$	β_4
5	$-\beta_5$	$-2\beta_4$	0	$-2\beta_4$	β_5

(2) We then calculate the chiral diagrams, using copy-free versions of Eq. (55) for the chiral operators, namely,

$$
\begin{aligned}
O_1^{xc;xd} &= \beta_1[(\sigma P^{(b)\dagger})_{x,c}(\sigma P^{(\bar{b})})_{x,d} \\
&\quad + (\sigma P^{*(b)\dagger}_\mu)_{x,c}(\sigma P^{*(\bar{b}),\mu})_{x,d}] \quad [\text{or } c \leftrightarrow d], \\
O_{2(3)}^{xc;xd} &= \beta_{2(3)}(\sigma P^{(b)\dagger})_{x,c}(\sigma P^{(\bar{b})})_{x,d} \\
&\quad + \beta'_{2(3)}(\sigma P^{*(b)\dagger}_\mu)_{x,c}(\sigma P^{*(\bar{b}),\mu})_{x,d} \quad [\text{or } c \leftrightarrow d], \\
O_{4(5)}^{xc;xd} &= \frac{\beta_{4(5)}}{2}[(\sigma P^{(b)\dagger})_{x,c}(\sigma^\dagger P^{(\bar{b})})_{x,d} \\
&\quad + (\sigma^\dagger P^{(b)\dagger})_{x,c}(\sigma P^{(\bar{b})})_{x,d}] \\
&\quad + \frac{\beta'_{4(5)}}{2}[(\sigma P^{*(b)\dagger}_\mu)_{x,c}(\sigma^\dagger P^{*(\bar{b}),\mu})_{x,d} \\
&\quad + (\sigma^\dagger P^{*(b)\dagger}_\mu)_{x,c}(\sigma P^{*(\bar{b}),\mu})_{x,d}] \quad [\text{or } c \leftrightarrow d].
\end{aligned}
\tag{57}
$$

The external interpolating fields are

$$P^{(b)}_{x,a} \quad \text{and} \quad P^{(\bar{b})\dagger}_{x,e}. \tag{58}$$

For a diagram with a given quark flow, one should use either the explicit version of the operators in Eq. (57) or the alternative $c \leftrightarrow d$ forms to ensure that the external taste-a light quark contracts with the taste-c light quark in the operators (which also guarantees that tastes e and d contract).

(3) Each diagram is then multiplied by the overall factor

$$F_\kappa \equiv \frac{1}{16N_\kappa}\sum_{t_\kappa}\Gamma^{\kappa,t_\kappa}_{ca}\Gamma^{\kappa,t_\kappa}_{de}, \tag{59}$$

and the repeated taste (a, c, d, e) and spin (κ) indices are summed.

B. Calculation

We are now ready to compute the one-loop diagrams in rHMSχPT using the Feynman rules given above in Eqs. (22) through (28) and Eq. (31). Because of the complications due to taste and copy indices, it is not possible in general simply to modify the continuum results of Ref. [11] to insert staggered corrections, as in Ref. [10]. We must calculate most chiral diagrams from scratch. The exception is the wave-function renormalization (parametrized below by the function $\mathcal{W}$), which is simple enough that the modification process ("staggering") works. In the wave-function case, the naive-to-staggered translation gives no complications because, from Eq. (41), it only requires setting initial and final tastes equal and averaging over them. The taste averaging has no effect because discrete taste symmetry (shift symmetry) implies that a two-point

FIG. 1. Meson-level tadpole graphs for the B-$\bar{B}$ mixing matrix element. In (a), the pion fields that are contracted both come from the same factor of σ in Eq. (57), while in (b) they come from different σ factors. For definiteness, we take the right external line in each diagram to be the incoming B meson, and the left external line, the outgoing $\bar{B}$. This means the left line is the contraction with the $P^{(b)\dagger}$ field in Eq. (57), while the right line is the contraction with the $P^{(\bar{b})}$ field. Diagram (a) is "factorizable" into a product of the left- and right-hand parts (the right-hand part is trivial here). Diagram (b) is "nonfactorizable." There is another diagram equivalent to (a) in which both pions come from the σ associated with the right-hand line.

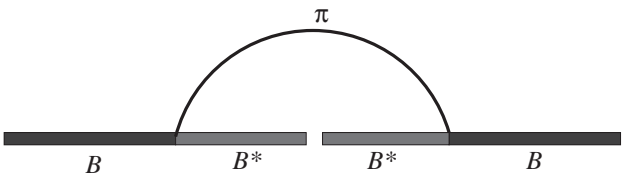

FIG. 2. The meson-level sunset graph for the B-$\bar{B}$ mixing matrix element. Conventions are as in Fig. 1.

function is in any case proportional to the identity in taste space.[3]

In addition to wave-function renormalization, there are two types of one-loop diagrams: tadpole graphs, Fig. 1, and sunset diagrams, Fig. 2. These are parametrized by functions $\mathcal{T}$ and $\mathcal{Q}$, respectively. Contributions from incorrect spins can enter in the tadpoles and sunset diagrams; we call such contributions $\tilde{\mathcal{T}}$, and $\tilde{\mathcal{Q}}$. The complete matrix elements are given by

$$\langle \bar{B}_x^0 | O_1^x | B_x^0 \rangle = \beta_1 \left(1 + \frac{\mathcal{W}_{x\bar{b}} + \mathcal{W}_{b\bar{x}}}{2} + \mathcal{T}_x^{(1)} + \tilde{\mathcal{T}}_x^{(1)} + \mathcal{Q}_x^{(1)} + \tilde{\mathcal{Q}}_x^{(1)} \right) + \text{analytic terms} \tag{60}$$

and

$$\langle \bar{B}_x^0 | O_n^x | B_x^0 \rangle = \beta_n \left(1 + \frac{\mathcal{W}_{x\bar{b}} + \mathcal{W}_{b\bar{x}}}{2} + \mathcal{T}_x^{(n)} + \tilde{\mathcal{T}}_x^{(n)} \right) + \beta_n' (\mathcal{Q}_x^{(n)} + \tilde{\mathcal{Q}}_x^{(n)}) + \text{analytic terms}, \tag{61}$$

for $n = 2, 3, 4, 5$. Nonrelativistic normalization, which is standard in heavy-light chiral perturbation theory, is assumed for the states $\langle \bar{B}_x^0 |$ and $| B_x^0 \rangle$ in these expressions. With relativistic normalization, an extra factor of M_{B_x}, the mass of the B_x meson, would appear on the right-hand sides.

In the partially quenched 2 + 1 ($m_u = m_d \neq m_s$) case, staggering the result for $\mathcal{W}_{q\bar{b}}$ in Ref. [11] gives

$$\mathcal{W}_{x\bar{b}} = \mathcal{W}_{b\bar{x}} = \frac{i g_{B^* B \pi}^2}{f_\pi^2} \left\{ \frac{1}{16} \sum_{\mathcal{S},\rho} N_\rho \mathcal{H}_{x\mathcal{S},\rho}^{\Delta^* + \delta_{\mathcal{S}x}} + \frac{1}{3} \left[R_{X_I}^{[2,2]}(\{M_{X_I}^{(2)}\}; \{\mu_I\}) \frac{\partial \mathcal{H}_{X,I}^{\Delta^*}}{\partial m_{X_I}^2} - \sum_{j \in \{M_I^{(2)}\}} D_{j,X_I}^{[2,2]}(\{M_{X_I}^{(2)}\}; \{\mu_I\}) \mathcal{H}_{j,I}^{\Delta^*} \right] \right.$$
$$\left. + a^2 \delta_V' \left[R_{X_V}^{[3,2]}(\{M_{X_V}^{(3)}\}; \{\mu_V\}) \frac{\partial \mathcal{H}_{X,V}^{\Delta^*}}{\partial m_{X_V}^2} - \sum_{j \in \{M_V^{(3)}\}} D_{j,X_V}^{[3,2]}(\{M_{X_V}^{(3)}\}; \{\mu_V\}) \mathcal{H}_{j,V}^{\Delta^*} \right] + (V \to A) \right\}, \tag{62}$$

where the index ρ runs over the taste representations (P,A, T,V,I) with degeneracies N_ρ, and $\mathcal{S}$ runs over the sea mesons u, d, s. The function $\mathcal{H}$ is equivalent to the integral $H(m, \Delta)$ defined in Eqs. (A3) and (A12) of Ref. [11]. The subscripts on $\mathcal{H}$ implicitly give the meson mass m in $H(m, \Delta)$ by specifying its flavor and taste. The flavor is indicated either by giving the flavor of the two quarks in the meson, as in $x\mathcal{S}$ in the first term in Eq. (62), or by giving the name of the meson, as in the remaining terms, where X refers to the meson made of two light valence quarks $x\bar{x}$ (m_X is its mass). The superscript on $\mathcal{H}$ is the second argument of the function $H(m, \Delta)$. It is the mass splitting between the heavy-light vector meson in the chiral loop and the external heavy-light pseudoscalar meson. In addition to the hyperfine splitting $\Delta^* = M_{B^*} - M_B$, it includes a light flavor splitting whenever the light flavor of

[3]With the exact momentum space taste construction [35], this statement is true to all orders in a, as can be seen most easily by using the formulation of shift symmetry in Ref. [19]. The construction is built into staggered chiral theory, so the statement is also true to all orders in rHMSχPT. The fact that we have used the (approximate) position space taste construction [9] in the translation from naive to staggered operators is irrelevant, since for our purposes only the lowest order translation is needed.

the vector meson in the loop is different from the the external flavor. For the first term in Eq. (62), the vector meson has flavor $\mathcal{S}$ so the splitting is $\delta_{\mathcal{S}x} \equiv M_{B_\mathcal{S}} - M_{B_x} = 2\lambda_1\mu(m_\mathcal{S} - m_x)$, where λ_1 and μ are low-energy constants. The constant λ_1 comes from heavy quark effective theory, and μ relates light meson masses to quark masses, Eq. (21).

For comparison, the function $\mathcal{H}$ is the same (up to constants) as the function J introduced in Ref. [7] [Eq. (6.17)]. Similarly the function $\mathcal{I}_{j,\rho}$ defined in [11] and used below is the same up to constants as the function $\ell(m^2_{j,\rho})$ used in Refs. [5,10,26]. The relations are

$$i\mathcal{H}^{\Delta}_{j,\rho} = -\frac{3}{16\pi^2} J(m_{j,\rho}, \Delta), \tag{63}$$

$$i\mathcal{I}_{j,\rho} = \frac{1}{16\pi^2}\ell(m^2_{j,\rho}) = \frac{1}{16\pi^2} m^2_{j,\rho} \ln(m^2_{j,\rho}/\Lambda^2_\chi). \tag{64}$$

In the limit of no splittings,

$$i\mathcal{H}^0_{j,\rho} = -3i\mathcal{I}_{j,\rho} = -\frac{3}{16\pi^2}\ell(m^2_{j,\rho}). \tag{65}$$

If one wants the B mixing result in the strict $1/m_B$ power counting in which the splittings are set to zero, one can simply use Eq. (65) for $\mathcal{H}$ everywhere below.

The (Euclidean) residue functions $R^{[n,k]}_j$ and $D^{[n,k]}_{j,l}$ in Eq. (62) are defined by [26]

$$\begin{aligned} R^{[n,k]}_j(\{m\},\{\mu\}) &\equiv \frac{\prod_{a=1}^k(\mu_a^2 - m_j^2)}{\prod_{i\neq j}(m_i^2 - m_j^2)}, \\ D^{[n,k]}_{j,l}(\{m\},\{\mu\}) &\equiv -\frac{d}{dm_l^2} R^{[n,k]}_j(\{m\},\{\mu\}). \end{aligned} \tag{66}$$

The mass combinations appearing as arguments of these functions in the 2 + 1 partially quenched theory are

$$\begin{aligned} \{M_X^{(2)}\} \equiv \{m_\eta, m_X\}, \quad \{M_X^{(3)}\} \equiv \{m_\eta, m_{\eta'}, m_X\}, \\ \{\mu\} \equiv \{m_l, m_h\}. \end{aligned} \tag{67}$$

The tastes of these mesons (I, V, or A) are indicated explicitly in Eq. (62).

The staggered heavy-light wave function renormalization is also calculated in Refs. [5,10] for the case where the heavy-meson splittings are neglected; the result of adding in those splittings as explained in Ref. [7] agrees with Eq. (62).

The tadpole and sunset contributions are more complicated, and we must follow the procedure outlined at the end of Sec. IV A. All four taste indices (two from the interpolating fields and two from the light quarks in the four-quark operator) enter in a nontrivial way, and shift symmetry does not require that all be equal. Indeed, taste symmetry violations arising ultimately from high-momentum gluon exchange can in general make one pair of tastes indices different from the other pair. However, if there are parts of a diagram that give simply a tree-level heavy-light propagator, the average over taste implied by Eq. (41) can suppress the taste-changing interactions. On the other hand, in some diagrams for wrong-spin contributions, the overall factor, Eq. (59), can project onto particular taste-violating internal pion propagators. The bottom line is that one must calculate the tadpole and sunset diagrams from first principles, and not simply try to stagger the continuum result.[4]

I start with the tadpoles. I call a diagram "connected" or "disconnected" based on whether the internal pion propagator is connected or disconnected in the quark flow sense of Eqs. (22) and (23) above. The only connected quark flow possible for Fig. 1(a) is shown in Fig. 3. This is a diagram with a sea quark loop; the sea quark has taste f, which is summed over. Taste conservation for the right-hand heavy-light propagator (the $P^{(\tilde{b})}P^{(\tilde{b})\dagger}$ propagator) gives a factor of δ_{de}. When combined with Eq. (59), this implies that $\Gamma_{\kappa,t_\kappa} = I$, so this diagram has no wrong-spin contributions. The taste factor from Eq. (22) is simply $\Gamma_{af}\Gamma_{fc} = \delta_{ac}$, which combines with the δ_{ca} from Eq. (59) (using $\Gamma_{\kappa,t_\kappa} = I$) to give a factor of 4. The sum over t_ρ then gives N_ρ, the degeneracy of representation ρ. Including the factor of 2 from the equivalent diagram with the loop on the right side of Fig. 3, and the factor of 1/4 for the rooted sea-quark loop, we get

$$\mathcal{T}^{(n)}_{x,\text{Fig.3}} = -\frac{i}{16F^2}\sum_{\rho,S} N_\rho \mathcal{I}_{xS,\rho}, \tag{68}$$

where $\mathcal{S}$ runs over the sea quarks u, d, s. Note that the result is independent of n. Since wrong-spin contributions to this diagram are absent, and $\beta^{(I)}_n = \beta_n$ for all n, Fig. 3 is simply proportional to β_n, which is factored out of $\mathcal{T}$ in Eqs. (60) and (61). The difference in chiral structure between the left-right operators $O_{4,5}$ and the left-left operators $O_{1,2,3}$ in Eq. (57) is not relevant because the even terms in the expansion of σ and $\sigma^\dagger$ are the same, and both π fields in Fig. 1(a) come from the same σ or $\sigma^\dagger$ factor.

There is also a disconnected contribution to Fig. 1(a). The quark flow diagram is shown in Fig. 4. Again the δ_{de} from the right-hand B propagator means that only the correct spin contributes. The taste factor from Eq. (23) is $\Gamma_{af}\Gamma_{fc} = \delta_{ac}$, which gives a factor 4 after using Eq. (59) and a factor of N_ρ from the sum over t_ρ. In this case only the I, V, and A channels contribute; see Eq. (25). In the singlet case, we can use the fact that $M^2_{\eta',I} \approx m_0^2$ for large

[4]The rules from Ref. [10] for staggering a continuum result would apply unchanged if, for example, we had set the two tastes in the four-quark operator equal and averaged over them, while either fixing the external tastes to any one value, or averaging over them. Such a definition of the operator could be arranged if we constructed point-split bilinears with the desired tastes within a hypercube, and then multiplied two of them appropriately. In that case, there would not be any wrong-spin contributions.

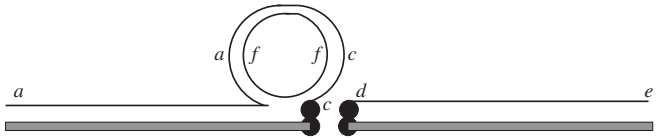

FIG. 3. Connected quark flow tadpole diagram. This is a contribution to Fig. 1(a). The thin lines denote staggered light quarks, and the thick, gray lines denote heavy quarks. Indices shown (a, f, c, d, e) are taste indices. The left pair of touching filled black circles represents the light and heavy quark in the $P^{(b)\dagger}$; the right pair represents the light and heavy quark in the $P^{(\bar{b})}$. Taste conservation for the right-hand B propagator forces $d = e$.

m_0, and take the limit $m_0 \to \infty$, resulting in one less pole in the denominator of Eq. (24) and an overall factor of $4/3$. In the vector and axial channels, we simply get a factor of 4 from N_ρ. This gives the standard ratio $1/3$ between the strength of the singlet and vector or axial hairpins, as seen in Ref. [10]. One may expect this standard ratio in any meson diagram, such as Fig. 1(a), that is unaffected by the complications from wrong spins or the naive-to-staggered translation. The result is

$$\begin{aligned}\mathcal{T}^{(n)}_{x,\mathrm{Fig.4}} = -\frac{i}{f^2}\Bigg\{&\frac{1}{3}\Bigg[R^{[2,2]}_{X_I}(\{M^{(2)}_{X_I}\};\{\mu_I\})\frac{\partial \mathcal{I}_{X,I}}{\partial m^2_{X_I}} \\ &- \sum_{j\in\{M^{(2)}_I\}} D^{[2,2]}_{j,X_I}(\{M^{(2)}_{X_I}\};\{\mu_I\})\mathcal{I}_{j,I}\Bigg] \\ &+ a^2\delta'_V\Bigg[R^{[3,2]}_{X_V}(\{M^{(3)}_{X_V}\};\{\mu_V\})\frac{\partial \mathcal{I}_{X,V}}{\partial m^2_{X_V}} \\ &- \sum_{j\in\{M^{(3)}_V\}} D^{[3,2]}_{j,X_V}(\{M^{(3)}_{X_V}\};\{\mu_V\})\mathcal{I}_{j,V}\Bigg] + (V\to A)\Bigg\}.\end{aligned} \tag{69}$$

Again, since wrong-spin contributions to this diagram are absent, the result is independent of n.

We now turn to contributions to the nonfactorizable diagram, Fig. 1(b). The connected contribution is shown in Fig. 5. This is the first diagram in which the quark flow connects the taste-a quark in the external $P^{(b)}_{x,a}$ field with the light quark in the $P^{(\bar{b})}$ field of the operator. According to the discussion above, this requires that we use the $c \leftrightarrow d$ versions of the operators in Eq. (57). The combination of taste matrices $\Gamma^{\rho,t_\rho}_{ad}\Gamma^{\rho,t_\rho}_{ec}$ from the connected propagator,

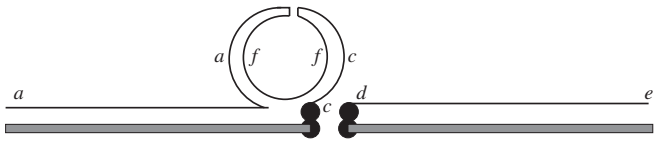

FIG. 4. Disconnected quark flow tadpole diagram. This is a contribution to Fig. 1(a). Taste conservation for the right-hand B propagator forces $d = e$.

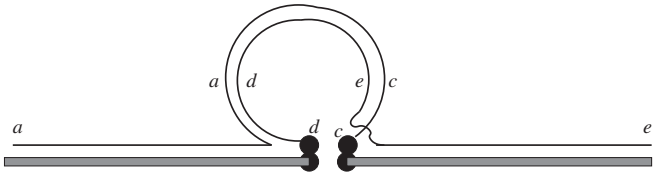

FIG. 5. Connected quark flow tadpole diagram. This is a contribution to Fig. 1(b). Taste violations on the connected pion line allow for $a \neq c$ and $d \neq e$.

Eq. (22), and $\Gamma^{\kappa,t_\kappa}_{ca}\Gamma^{\kappa,t_\kappa}_{de}$ from the overall factor, Eq. (59), appears in several diagrams. It is therefore useful to define

$$\zeta(\kappa,\rho) = \frac{1}{4N_\kappa N_\rho}\sum_{t_\kappa,t_\rho}\mathrm{tr}(\Gamma^{\kappa,t_\kappa}\Gamma^{\rho,t_\rho}\Gamma^{\kappa,t_\kappa}\Gamma^{\rho,t_\rho}). \tag{70}$$

The factors of N_κ and N_ρ have been included in the denominator for later convenience. Completeness of the 16 matrices Γ^{κ,t_κ} implies that ζ satisfies the normalization condition,

$$\sum_\kappa N_\kappa\zeta(\kappa,\rho) = 16\delta_{\rho,I}. \tag{71}$$

Values of $\zeta(\kappa,\rho)$ are given in Table II.

In terms of $\zeta(\kappa,\rho)$, the correct-spin and wrong-spin contributions of Fig. 5 are then

$$\mathcal{T}^{(n)}_{x,\mathrm{Fig.5}} = \mp\frac{i}{16f^2}\sum_\rho N_\rho\mathcal{I}_{X,\rho}, \tag{72}$$

$$\tilde{\mathcal{T}}^{(n)}_{x,\mathrm{Fig.5}} = \mp\frac{i}{16f^2}\sum_{\kappa\neq I}\left(\frac{\beta^{(\kappa)}_n}{\beta_n}\sum_\rho N_\rho\zeta(\kappa,\rho)\mathcal{I}_{X,\rho}\right), \tag{73}$$

where the upper sign is for $n = 1, 2, 3$ and the lower sign is for $n = 4, 5$. The difference in chiral structure of Eq. (57) between $O^x_{4,5}$ and $O^x_{1,2,3}$ in Eq. (57) matters for Fig. 1(b), because the two pion fields come from different σ or $\sigma^\dagger$ factors. The correct-spin contribution $\mathcal{T}^{(n)}_{x,\mathrm{Fig.5}}$ comes from the $\kappa = I$ term in the sum, while the $\kappa \neq I$ terms give the wrong-spin piece $\tilde{\mathcal{T}}^{(n)}_{x,\mathrm{Fig.5}}$. The quantities $\beta^{(\kappa)}_n$ are listed in Table I.

The final tadpole diagram is the disconnected contribution to Fig. 1(b), shown in Fig. 6. In this case, the taste structure of the disconnected propagator Eq. (23) is $\Gamma^{\rho,t_\rho}_{ac}\Gamma^{\rho,t_\rho}_{ed}$, which, when combined with the taste matrices

TABLE II. Matrix of $\zeta(\kappa,\rho)$ values.

	P	A	T	V	I
P	1	-1	1	-1	1
A	-1	$-1/2$	0	$1/2$	1
T	1	0	$-1/3$	0	1
V	-1	$1/2$	0	$-1/2$	1
I	1	1	1	1	1

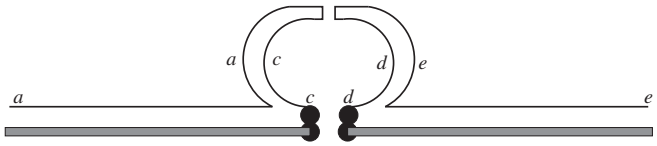

FIG. 6. Disconnected quark flow tadpole diagram. This is a contribution to Fig. 1(b). Taste-violating hairpins allow $a \neq c$ and $d \neq e$.

in the overall factor, Eq. (59), gives $\mathrm{tr}^2(\Gamma^{\kappa,t_\kappa}\Gamma^{\rho,t_\rho}) = 16\delta_{\kappa\rho}\delta_{t_\kappa t_\rho}$. The hairpin propagator is nonzero only in the I, V, and A channels. So we get a singlet contribution to the correct-spin operator ($\kappa = \rho = I$) and taste-violating contributions for two of the wrong-spin operators ($\kappa = \rho = V, A$). The result is

$$\mathcal{T}^{(n)}_{x,\mathrm{Fig.6}} = \mp\frac{i}{3f^2}\Big\{R^{[2,2]}_{X_I}(\{M^{(2)}_{X_I}\};\{\mu_I\})\frac{\partial \mathcal{I}_{X,I}}{\partial m^2_{X_I}} - \sum_{j\in\{M^{(2)}_I\}} D^{[2,2]}_{j,X_I}(\{M^{(2)}_{X_I}\};\{\mu_I\})\mathcal{I}_{j,I}\Big\}, \tag{74}$$

$$\begin{aligned}\tilde{\mathcal{T}}^{(n)}_{x,\mathrm{Fig.6}} = \mp\frac{i}{4\beta_n f^2}\Big\{&\beta^{(V)}_n a^2\delta'_V\Big[R^{[3,2]}_{X_V}(\{M^{(3)}_{X_V}\};\{\mu_V\})\frac{\partial \mathcal{I}_{X,V}}{\partial m^2_{X_V}} - \sum_{j\in\{M^{(3)}_V\}} D^{[3,2]}_{j,X_V}(\{M^{(3)}_{X_V}\};\{\mu_V\})\mathcal{I}_{j,V}\Big]\\ &+\beta^{(A)}_n a^2\delta'_A\Big[R^{[3,2]}_{X_A}(\{M^{(3)}_{X_A}\};\{\mu_A\})\frac{\partial \mathcal{I}_{X,A}}{\partial m^2_{X_A}} - \sum_{j\in\{M^{(3)}_A\}} D^{[3,2]}_{j,X_A}(\{M^{(3)}_{X_A}\};\{\mu_A\})\mathcal{I}_{j,A}\Big]\Big\}.\end{aligned} \tag{75}$$

Again the upper sign is for $n = 1, 2, 3$ and the lower sign is for $n = 4, 5$; the reasoning is the same as in Eqs. (72) and (73).

The sunset diagram, Fig. 2, is very similar to the tadpole contribution that connects the incoming B and outgoing $\bar{B}$, Fig. 1(b). Again, there are two quark flows: Fig. 7, a connected graph similar to Fig. 5, and Fig. 8, a disconnected graph similar to Fig. 6. The taste structures of the sunset graphs are identical to the corresponding tadpole graphs. As in Fig. 5, the $c \leftrightarrow d$ version of Eq. (57) is used in Fig. 7. The main difference between the sunset and tadpole graphs is the actual integral, which here involves two heavy-light propagators and factors of $g_{B^*B\pi}$, and so gives $g^2_{B^*B\pi}\mathcal{H}^{\Delta^*}$ instead of $\mathcal{I}$. In addition, the σ and $\sigma^\dagger$ matrices in Eq. (57) are all set to 1 in the sunset case, so there is no difference in overall sign between the results for operators 1, 2, 3 and those for operators 4, 5. Otherwise, everything is the same as for the tadpole case. I find, for Fig. 7,

$$\mathcal{Q}^{(n)}_{x,\mathrm{Fig.7}} = -\frac{ig^2_{B^*B\pi}}{16f^2}\sum_\rho N_\rho \mathcal{H}^{\Delta^*}_{X,\rho}, \tag{76}$$

$$\tilde{\mathcal{Q}}^{(n)}_{x,\mathrm{Fig.7}} = -\frac{ig^2_{B^*B\pi}}{16f^2}\sum_{\kappa\neq I}\Big(\frac{\beta^{\prime(\kappa)}_n}{\beta'_n}\sum_\rho N_\rho\zeta(\kappa,\rho)\mathcal{H}^{\Delta^*}_{X,\rho}\Big). \tag{77}$$

The disconnected sunset graph, Fig. 8, gives

$$\mathcal{Q}^{(n)}_{x,\mathrm{Fig.8}} = \frac{-ig^2_{B^*B\pi}}{3f^2}\Big\{R^{[2,2]}_{X_I}(\{M^{(2)}_{X_I}\};\{\mu_I\})\frac{\partial \mathcal{H}^{\Delta^*}_{X,I}}{\partial m^2_{X_I}} - \sum_{j\in\{M^{(2)}_I\}} D^{[2,2]}_{j,X_I}(\{M^{(2)}_{X_I}\};\{\mu_I\})\mathcal{H}^{\Delta^*}_{j,I}\Big\}, \tag{78}$$

$$\begin{aligned}\tilde{\mathcal{Q}}^{(n)}_{x,\mathrm{Fig.8}} = -\frac{ig^2_{B^*B\pi}}{4\beta'_n f^2}\Big\{&\beta^{\prime(V)}_n a^2\delta'_V\Big[R^{[3,2]}_{X_V}(\{M^{(3)}_{X_V}\};\{\mu_V\})\\ &\times\frac{\partial \mathcal{H}^{\Delta^*}_{X,V}}{\partial m^2_{X_V}} - \sum_{j\in\{M^{(3)}_V\}} D^{[3,2]}_{j,X_V}(\{M^{(3)}_{X_V}\};\{\mu_V\})\mathcal{H}^{\Delta^*}_{j,V}\Big]\\ &+\beta^{\prime(A)}_n a^2\delta'_A\Big[R^{[3,2]}_{X_A}(\{M^{(3)}_{X_A}\};\{\mu_A\})\frac{\partial \mathcal{H}^{\Delta^*}_{X,A}}{\partial m^2_{X_A}} - \sum_{j\in\{M^{(3)}_A\}} D^{[3,2]}_{j,X_A}(\{M^{(3)}_{X_A}\};\{\mu_A\})\mathcal{H}^{\Delta^*}_{j,A}\Big]\Big\}.\end{aligned} \tag{79}$$

C. Other possible taste-breaking contributions

Under renormalization, there are continuum-like mixings of the desired four-quark lattice operators [38], but there may in addition be perturbative mixing with operators of incorrect spin and taste. Further, there are discretization corrections to our identification of the spin and taste of the operators, which can arise from variations in the heavy-quark field over a spatial cube, as well as higher order terms in the position-space spin-taste formalism [9]. However, incorrect spin-taste operators generated by any of these causes cannot contribute to nonanalytic terms in the matrix element until NNLO.

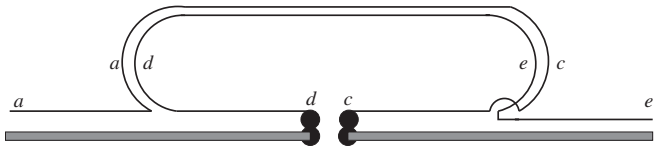

FIG. 7. Connected quark flow sunset graph corresponding to Fig. 2. Taste violations on the connected pion line allow for $a \neq c$ and $d \neq e$.

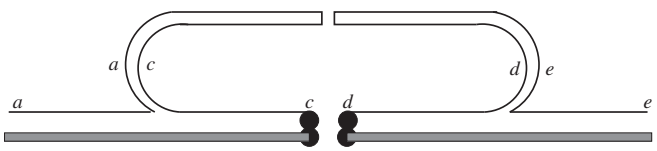

FIG. 8. Disconnected (hairpin) quark flow sunset graphs corresponding to Fig. 2. Taste-violating hairpins allow for $a \neq c$ and $d \neq e$.

In order to see this, consider the standard power counting in (rooted) staggered chiral perturbation theory (rSχPT):

$$p^2 \sim m \sim a^2. \tag{80}$$

The B^0–$\bar{B}^0$ mixing four-fermion operators, when translated into the chiral effective theory, are of $\mathcal{O}(1)$ in the aforementioned power-counting scheme. Thus their LO (tree-level) contributions to the relevant matrix elements are of $\mathcal{O}(1)$, and their NLO (one-loop) contributions are of $\mathcal{O}(p^2)$.

Perturbative mixing with wrong-taste operators can occur at one-loop order in α_S. In the chiral effective theory, these wrong-taste operators would thus enter with coefficients of $\mathcal{O}(\alpha_S/4\pi)$. As was shown in Ref. [39], which considered the contribution of wrong-taste operators to neutral kaon mixing in rSχPT, $\alpha_S/4\pi$ is numerically of the same size as the taste-breaking factor $a^2\alpha_S^2$ on the $a \approx 0.12$ fm MILC Asqtad ensembles [23]. Thus the appropriate way to include the strong coupling constant in the rHMSχPT power counting is

$$p^2 \sim m \sim a^2 \sim \alpha_S/4\pi. \tag{81}$$

One-loop chiral diagrams involving the wrong-taste operators from perturbative mixing would therefore contribute to matrix elements only at NNLO, $\mathcal{O}(\alpha_S/4\pi p^2)$, higher order than I am considering here.

Wrong-taste operators may also occur because of the $\mathcal{O}(a)$ corrections to the taste identification of the operators and the interpolating fields, Eqs. (40) and (44), coming either from the variation of the heavy quark field over the hypercube [see Eq. (36)] or from $\mathcal{O}(a)$ corrections to spin-taste identification of Eq. (38). Since the matrix elements are taste conserving at tree level in rHMSχPT, any such taste-violating effects must appear twice, inducing $\mathcal{O}(a^2)$ corrections. These effects can then be absorbed into a^2-dependent analytic terms [see Eq. (95) below]. Nontrivial terms could appear at one loop in chiral perturbation theory, but the extra factor of a^2 implies that such terms are again effectively NNLO.

Consequently, only the LO taste breaking in the four-quark operators, together with taste-breaking terms in the LO pion chiral Lagrangian, will modify the one-loop continuum chiral logarithms, and these modifications are what have been calculated above. Note however, that in more highly improved versions of staggered quarks, taste violations [the a^2 terms in Eq. (81)] will be reduced relative to the Asqtad case, but perturbative mixing may not be similarly reduced. In such cases, it may be more reasonable to consider the $\mathcal{O}(\alpha_S)$ perturbative corrections to be of LO in the chiral expansion, and their one-loop chiral corrections to be NLO, the same order as the corrections computed in Sec. IV B. I make some more comments on this point in Sec. VI.

V. FINAL RESULTS

We can now combine results from different graphs to get the complete tadpole and sunset contributions. For the correct-spin tadpole contribution, adding Eqs. (68), (69), (72), and (74) gives

$$\begin{aligned}\mathcal{T}_x^{(1,2,3)} = \frac{-i}{f_\pi^2}\Bigg\{&\frac{1}{16}\sum_{\mathcal{S},\rho} N_\rho \mathcal{I}_{x\mathcal{S},\rho} + \frac{1}{16}\sum_{\rho} N_\rho \mathcal{I}_{X,\rho} + \frac{2}{3}\Bigg[R_{X_I}^{[2,2]}(\{M_{X_I}^{(2)}\};\{\mu_I\})\frac{\partial \mathcal{I}_{X,I}}{\partial m_{X_I}^2} - \sum_{j\in\{M_I^{(2)}\}} D_{j,X_I}^{[2,2]}(\{M_{X_I}^{(2)}\};\{\mu_I\})\mathcal{I}_{j,I}\Bigg] \\ &+ a^2\delta'_V\Bigg[R_{X_V}^{[3,2]}(\{M_{X_V}^{(3)}\};\{\mu_V\})\frac{\partial \mathcal{I}_{X,V}}{\partial m_{X_V}^2} - \sum_{j\in\{M_V^{(3)}\}} D_{j,X_V}^{[3,2]}(\{M_{X_V}^{(3)}\};\{\mu_V\})\mathcal{I}_{j,V}\Bigg] + (V\to A)\Bigg\},\end{aligned} \tag{82}$$

$$\mathcal{T}_x^{(4,5)} = \frac{-i}{f_\pi^2}\Bigg\{\frac{1}{16}\sum_{\mathcal{S},\rho} N_\rho \mathcal{I}_{x\mathcal{S},\rho} - \frac{1}{16}\sum_{\rho} N_\rho \mathcal{I}_{X,\rho} + a^2\delta'_V\Bigg[R_{X_V}^{[3,2]}(\{M_{X_V}^{(3)}\};\{\mu_V\})\frac{\partial \mathcal{I}_{X,V}}{\partial m_{X_V}^2} - \sum_{j\in\{M_V^{(3)}\}} D_{j,X_V}^{[3,2]}(\{M_{X_V}^{(3)}\};\{\mu_V\})\mathcal{I}_{j,V}\Bigg] + (V\to A)\Bigg\}. \tag{83}$$

The incorrect-spin tadpole contributions come from Eqs. (73) and (75). Adding them, and using the values of $\beta_n^{(\kappa)}$ in Table I and of $\zeta(\kappa,\rho)$ in Table II, we have

$$\begin{aligned}\tilde{\mathcal{T}}_x^{(1)} = \frac{-i}{f_\pi^2}\Bigg\{&\frac{1}{16}(-5\mathcal{I}_{X,P} - 4\mathcal{I}_{X,A} + 18\mathcal{I}_{X,T} - 4\mathcal{I}_{X,V} - 5\mathcal{I}_{X,I}) \\ &+ \frac{2(\beta_2+\beta_3)}{\beta_1}\Bigg(-\mathcal{I}_{X,V} + \mathcal{I}_{X,A} + a^2\delta'_V\Bigg[R_{X_V}^{[3,2]}(\{M_{X_V}^{(3)}\};\{\mu_V\})\frac{\partial \mathcal{I}_{X,V}}{\partial m_{X_V}^2} - \sum_{j\in\{M_V^{(3)}\}} D_{j,X_V}^{[3,2]}(\{M_{X_V}^{(3)}\};\{\mu_V\})\mathcal{I}_{j,V}\Bigg] \\ &- a^2\delta'_A\Bigg[R_{X_A}^{[3,2]}(\{M_{X_A}^{(3)}\};\{\mu_A\})\frac{\partial \mathcal{I}_{X,A}}{\partial m_{X_A}^2} - \sum_{j\in\{M_A^{(3)}\}} D_{j,X_A}^{[3,2]}(\{M_{X_A}^{(3)}\};\{\mu_A\})\mathcal{I}_{j,A}\Bigg]\Bigg)\Bigg\},\end{aligned} \tag{84}$$

$$\tilde{\mathcal{T}}_x^{(2)} = \frac{-i}{f_\pi^2}\Big\{\frac{1}{16}(-\mathcal{I}_{X,P} - 4\mathcal{I}_{X,A} + 10\mathcal{I}_{X,T} - 4\mathcal{I}_{X,V} - \mathcal{I}_{X,I}) + \frac{\beta_3}{4\beta_2}(-\mathcal{I}_{X,P} + 2\mathcal{I}_{X,T} - \mathcal{I}_{X,I}) + \frac{\beta_1}{4\beta_2}\Big(-\mathcal{I}_{X,V} + \mathcal{I}_{X,A} + a^2\delta'_V\Big[R^{[3,2]}_{X_V}(\{M^{(3)}_{X_V}\};\{\mu_V\})\frac{\partial \mathcal{I}_{X,V}}{\partial m^2_{X_V}} - \sum_{j\in\{M^{(3)}_V\}} D^{[3,2]}_{j,X_V}(\{M^{(3)}_{X_V}\};\{\mu_V\})\mathcal{I}_{j,V}\Big] - a^2\delta'_A\Big[R^{[3,2]}_{X_A}(\{M^{(3)}_{X_A}\};\{\mu_A\})\frac{\partial \mathcal{I}_{X,A}}{\partial m^2_{X_A}} - \sum_{j\in\{M^{(3)}_A\}} D^{[3,2]}_{j,X_A}(\{M^{(3)}_{X_A}\};\{\mu_A\})\mathcal{I}_{j,A}\Big]\Big)\Big\}, \tag{85}$$

$$\tilde{\mathcal{T}}_x^{(3)} = \frac{-i}{f_\pi^2}\Big\{\frac{1}{16}(-\mathcal{I}_{X,P} - 4\mathcal{I}_{X,A} + 10\mathcal{I}_{X,T} - 4\mathcal{I}_{X,V} - \mathcal{I}_{X,I}) + \frac{\beta_2}{4\beta_3}(-\mathcal{I}_{X,P} + 2\mathcal{I}_{X,T} - \mathcal{I}_{X,I}) + \frac{\beta_1}{4\beta_3}\Big(-\mathcal{I}_{X,V} + \mathcal{I}_{X,A} + a^2\delta'_V\Big[R^{[3,2]}_{X_V}(\{M^{(3)}_{X_V}\};\{\mu_V\})\frac{\partial \mathcal{I}_{X,V}}{\partial m^2_{X_V}} - \sum_{j\in\{M^{(3)}_V\}} D^{[3,2]}_{j,X_V}(\{M^{(3)}_{X_V}\};\{\mu_V\})\mathcal{I}_{j,V}\Big] - a^2\delta'_A\Big[R^{[3,2]}_{X_A}(\{M^{(3)}_{X_A}\};\{\mu_A\})\frac{\partial \mathcal{I}_{X,A}}{\partial m^2_{X_A}} - \sum_{j\in\{M^{(3)}_A\}} D^{[3,2]}_{j,X_A}(\{M^{(3)}_{X_A}\};\{\mu_A\})\mathcal{I}_{j,A}\Big]\Big)\Big\}, \tag{86}$$

$$\tilde{\mathcal{T}}_x^{(4)} = \frac{i}{f_\pi^2}\Big\{\frac{1}{16}(-\mathcal{I}_{X,P} + 4\mathcal{I}_{X,A} - 6\mathcal{I}_{X,T} + 4\mathcal{I}_{X,V} - \mathcal{I}_{X,I}) + \frac{\beta_5}{4\beta_4}\Big(\mathcal{I}_{X,P} - \mathcal{I}_{X,I} - 2a^2\delta'_V\Big[R^{[3,2]}_{X_V}(\{M^{(3)}_{X_V}\};\{\mu_V\})\frac{\partial \mathcal{I}_{X,V}}{\partial m^2_{X_V}} - \sum_{j\in\{M^{(3)}_V\}} D^{[3,2]}_{j,X_V}(\{M^{(3)}_{X_V}\};\{\mu_V\})\mathcal{I}_{j,V}\Big] - 2a^2\delta'_A\Big[R^{[3,2]}_{X_A}(\{M^{(3)}_{X_A}\};\{\mu_A\})\frac{\partial \mathcal{I}_{X,A}}{\partial m^2_{X_A}} - \sum_{j\in\{M^{(3)}_A\}} D^{[3,2]}_{j,X_A}(\{M^{(3)}_{X_A}\};\{\mu_A\})\mathcal{I}_{j,A}\Big]\Big)\Big\}, \tag{87}$$

$$\tilde{\mathcal{T}}_x^{(5)} = \frac{i}{f_\pi^2}\Big\{\frac{1}{16}(-\mathcal{I}_{X,P} + 4\mathcal{I}_{X,A} - 6\mathcal{I}_{X,T} + 4\mathcal{I}_{X,V} - \mathcal{I}_{X,I}) + \frac{\beta_4}{4\beta_5}\Big(\mathcal{I}_{X,P} - \mathcal{I}_{X,I} - 2a^2\delta'_V\Big[R^{[3,2]}_{X_V}(\{M^{(3)}_{X_V}\};\{\mu_V\})\frac{\partial \mathcal{I}_{X,V}}{\partial m^2_{X_V}} - \sum_{j\in\{M^{(3)}_V\}} D^{[3,2]}_{j,X_V}(\{M^{(3)}_{X_V}\};\{\mu_V\})\mathcal{I}_{j,V}\Big] - 2a^2\delta'_A\Big[R^{[3,2]}_{X_A}(\{M^{(3)}_{X_A}\};\{\mu_A\})\frac{\partial \mathcal{I}_{X,A}}{\partial m^2_{X_A}} - \sum_{j\in\{M^{(3)}_A\}} D^{[3,2]}_{j,X_A}(\{M^{(3)}_{X_A}\};\{\mu_A\})\mathcal{I}_{j,A}\Big]\Big)\Big\}. \tag{88}$$

In the continuum limit, when all taste propagators become degenerate and $a^2\delta'_{V,A} \to 0$, the wrong-spin terms clearly vanish.

For the correct-spin sunset diagrams, adding Eqs. (76) and (78) gives

$$\mathcal{Q}_x^{(n)} = \frac{-ig^2_{B^*B\pi}}{f_\pi^2}\Big\{\frac{1}{16}\sum_\rho N_\rho \mathcal{H}^{\Delta^*}_{X,\rho} + \frac{1}{3}\Big[R^{[2,2]}_{X_I}(\{M^{(2)}_{X_I}\};\{\mu_I\})\frac{\partial \mathcal{H}^{\Delta^*}_{X,I}}{\partial m^2_{X_I}} - \sum_{j\in\{M^{(2)}_I\}} D^{[2,2]}_{j,X_I}(\{M^{(2)}_{X_I}\};\{\mu_I\})\mathcal{H}^{\Delta^*}_{j,I}\Big]\Big\}. \tag{89}$$

The incorrect-spin sunset contributions come from Eqs. (77) and (79). Again using the values of $\zeta(\kappa, \rho)$ in Table II and of $\beta_n^{(\kappa)}$ in Table I, we have

$$\tilde{\mathcal{Q}}_x^{(1)} = \frac{-ig^2_{B^*B\pi}}{f_\pi^2}\Big\{\frac{1}{16}(-5\mathcal{H}^{\Delta^*}_{X,P} - 4\mathcal{H}^{\Delta^*}_{X,A} + 18\mathcal{H}^{\Delta^*}_{X,T} - 4\mathcal{H}^{\Delta^*}_{X,V} - 5\mathcal{H}^{\Delta^*}_{X,I}) + \frac{2(\beta_2' + \beta_3')}{\beta_1}\Big(-\mathcal{H}^{\Delta^*}_{X,V} + \mathcal{H}^{\Delta^*}_{X,A} + a^2\delta_V'\Big[R^{[3,2]}_{X_V}(\{M^{(3)}_{X_V}\};\{\mu_V\})\frac{\partial \mathcal{H}^{\Delta^*}_{X,V}}{\partial m^2_{X_V}} - \sum_{j\in\{M_V^{(3)}\}} D^{[3,2]}_{j,X_V}(\{M^{(3)}_{X_V}\};\{\mu_V\})\mathcal{H}^{\Delta^*}_{j,V}\Big] - a^2\delta_A'\Big[R^{[3,2]}_{X_A}(\{M^{(3)}_{X_A}\};\{\mu_A\})\frac{\partial \mathcal{H}^{\Delta^*}_{X,A}}{\partial m^2_{X_A}} - \sum_{j\in\{M_A^{(3)}\}} D^{[3,2]}_{j,X_A}(\{M^{(3)}_{X_A}\};\{\mu_A\})\mathcal{H}^{\Delta^*}_{j,A}\Big]\Big)\Big\}, \tag{90}$$

$$\tilde{\mathcal{Q}}_x^{(2)} = \frac{-ig^2_{B^*B\pi}}{f_\pi^2}\Big\{\frac{1}{16}(-\mathcal{H}^{\Delta^*}_{X,P} - 4\mathcal{H}^{\Delta^*}_{X,A} + 10\mathcal{H}^{\Delta^*}_{X,T} - 4\mathcal{H}^{\Delta^*}_{X,V} - \mathcal{H}^{\Delta^*}_{X,I}) + \frac{\beta_3'}{4\beta_2'}(-\mathcal{H}^{\Delta^*}_{X,P} + 2\mathcal{H}^{\Delta^*}_{X,T} - \mathcal{H}^{\Delta^*}_{X,I}) + \frac{\beta_1}{4\beta_2'}\Big(-\mathcal{H}^{\Delta^*}_{X,V} + \mathcal{H}^{\Delta^*}_{X,A} + a^2\delta_V'\Big[R^{[3,2]}_{X_V}(\{M^{(3)}_{X_V}\};\{\mu_V\})\frac{\partial \mathcal{H}^{\Delta^*}_{X,V}}{\partial m^2_{X_V}} - \sum_{j\in\{M_V^{(3)}\}} D^{[3,2]}_{j,X_V}(\{M^{(3)}_{X_V}\};\{\mu_V\})\mathcal{H}^{\Delta^*}_{j,V}\Big] - a^2\delta_A'\Big[R^{[3,2]}_{X_A}(\{M^{(3)}_{X_A}\};\{\mu_A\})\frac{\partial \mathcal{H}^{\Delta^*}_{X,A}}{\partial m^2_{X_A}} - \sum_{j\in\{M_A^{(3)}\}} D^{[3,2]}_{j,X_A}(\{M^{(3)}_{X_A}\};\{\mu_A\})\mathcal{H}^{\Delta^*}_{j,A}\Big]\Big)\Big\}, \tag{91}$$

$$\tilde{\mathcal{Q}}_x^{(3)} = \frac{-ig^2_{B^*B\pi}}{f_\pi^2}\Big\{\frac{1}{16}(-\mathcal{H}^{\Delta^*}_{X,P} - 4\mathcal{H}^{\Delta^*}_{X,A} + 10\mathcal{H}^{\Delta^*}_{X,T} - 4\mathcal{H}^{\Delta^*}_{X,V} - \mathcal{H}^{\Delta^*}_{X,I}) + \frac{\beta_2'}{4\beta_3'}(-\mathcal{H}^{\Delta^*}_{X,P} + 2\mathcal{H}^{\Delta^*}_{X,T} - \mathcal{H}^{\Delta^*}_{X,I}) + \frac{\beta_1}{4\beta_3'}\Big(-\mathcal{H}^{\Delta^*}_{X,V} + \mathcal{H}^{\Delta^*}_{X,A} + a^2\delta_V'\Big[R^{[3,2]}_{X_V}(\{M^{(3)}_{X_V}\};\{\mu_V\})\frac{\partial \mathcal{H}^{\Delta^*}_{X,V}}{\partial m^2_{X_V}} - \sum_{j\in\{M_V^{(3)}\}} D^{[3,2]}_{j,X_V}(\{M^{(3)}_{X_V}\};\{\mu_V\})\mathcal{H}^{\Delta^*}_{j,V}\Big] - a^2\delta_A'\Big[R^{[3,2]}_{X_A}(\{M^{(3)}_{X_A}\};\{\mu_A\})\frac{\partial \mathcal{H}^{\Delta^*}_{X,A}}{\partial m^2_{X_A}} - \sum_{j\in\{M_A^{(3)}\}} D^{[3,2]}_{j,X_A}(\{M^{(3)}_{X_A}\};\{\mu_A\})\mathcal{H}^{\Delta^*}_{j,A}\Big]\Big)\Big\}, \tag{92}$$

$$\tilde{\mathcal{Q}}_x^{(4)} = \frac{-ig^2_{B^*B\pi}}{f_\pi^2}\Big\{\frac{1}{16}(-\mathcal{H}^{\Delta^*}_{X,P} + 4\mathcal{H}^{\Delta^*}_{X,A} - 6\mathcal{H}^{\Delta^*}_{X,T} + 4\mathcal{H}^{\Delta^*}_{X,V} - \mathcal{H}^{\Delta^*}_{X,I}) + \frac{\beta_5'}{4\beta_4'}\Big(\mathcal{H}^{\Delta^*}_{X,P} - \mathcal{H}^{\Delta^*}_{X,I} - 2a^2\delta_V'\Big[R^{[3,2]}_{X_V}(\{M^{(3)}_{X_V}\};\{\mu_V\})\frac{\partial \mathcal{H}^{\Delta^*}_{X,V}}{\partial m^2_{X_V}} - \sum_{j\in\{M_V^{(3)}\}} D^{[3,2]}_{j,X_V}(\{M^{(3)}_{X_V}\};\{\mu_V\})\mathcal{H}^{\Delta^*}_{j,V}\Big] - 2a^2\delta_A'\Big[R^{[3,2]}_{X_A}(\{M^{(3)}_{X_A}\};\{\mu_A\})\frac{\partial \mathcal{H}^{\Delta^*}_{X,A}}{\partial m^2_{X_A}} - \sum_{j\in\{M_A^{(3)}\}} D^{[3,2]}_{j,X_A}(\{M^{(3)}_{X_A}\};\{\mu_A\})\mathcal{H}^{\Delta^*}_{j,A}\Big]\Big)\Big\}, \tag{93}$$

$$\tilde{\mathcal{Q}}_x^{(5)} = \frac{-ig^2_{B^*B\pi}}{f_\pi^2}\Big\{\frac{1}{16}(-\mathcal{H}^{\Delta^*}_{X,P} + 4\mathcal{H}^{\Delta^*}_{X,A} - 6\mathcal{H}^{\Delta^*}_{X,T} + 4\mathcal{H}^{\Delta^*}_{X,V} - \mathcal{H}^{\Delta^*}_{X,I}) + \frac{\beta_4'}{4\beta_5'}\Big(\mathcal{H}^{\Delta^*}_{X,P} - \mathcal{H}^{\Delta^*}_{X,I} - 2a^2\delta_V'\Big[R^{[3,2]}_{X_V}(\{M^{(3)}_{X_V}\};\{\mu_V\})\frac{\partial \mathcal{H}^{\Delta^*}_{X,V}}{\partial m^2_{X_V}} - \sum_{j\in\{M_V^{(3)}\}} D^{[3,2]}_{j,X_V}(\{M^{(3)}_{X_V}\};\{\mu_V\})\mathcal{H}^{\Delta^*}_{j,V}\Big] - 2a^2\delta_A'\Big[R^{[3,2]}_{X_A}(\{M^{(3)}_{X_A}\};\{\mu_A\})\frac{\partial \mathcal{H}^{\Delta^*}_{X,A}}{\partial m^2_{X_A}} - \sum_{j\in\{M_A^{(3)}\}} D^{[3,2]}_{j,X_A}(\{M^{(3)}_{X_A}\};\{\mu_A\})\mathcal{H}^{\Delta^*}_{j,A}\Big]\Big)\Big\}. \tag{94}$$

In comparing Eqs. (62), (82), (83), and (89) to the continuum results of Ref. [11], one needs to be aware of the many differences in notation. In particular, the particles called X and π in Ref. [11] are called η and X, respectively, here. Taking the notational differences into account, it is straightforward to check that the continuum limits of the above equations reproduce the results in Ref. [11].

The analytic terms in Eqs. (60) and (61) are of the form

$$\text{analytic terms} = L_v^{(n)} m_x + L_s^{(n)}(2m_l + m_h) + L_a^{(n)} a^2, \tag{95}$$

where $L_v^{(n)}$ and $L_s^{(n)}$ are continuum low-energy constants, and $L_a^{(n)}$ are lattice low-energy constants, summarizing the effects of taste-violating analytic chiral operators at NLO. As indicated, these constants depend on n, i.e., on the operator whose matrix element is being calculated. It is straightforward to see that these are in fact the analytic terms that may appear by considering the effects of adding mass or taste-violating spurions to the chiral operators in Eq. (57). The parameters $L_v^{(n)}$, $L_s^{(n)}$, and $L_a^{(n)}$, together with the parameters $\hat{\beta}_n$ and $\hat{\beta}'_n$ in Eqs. (60) and (61) are to be determined from the fits to lattice data.

VI. CONCLUSIONS AND DISCUSSION

I have calculated neutral B mixing to one-loop in staggered chiral perturbation theory for the complete set of standard model and beyond-the-standard-model operators, Eq. (1). My results are given by Eqs. (60) and (61), with expressions for the various terms listed in Eqs. (62) and (82) through (95).

The construction of the operators on the lattice as local products of local heavy-light bilinears, coupled with the use of staggered light quarks, results in the appearance of "wrong spin/taste operators" that are $\mathcal{O}(1)$ in the lattice spacing. Their contributions to the matrix elements considered here are suppressed to NLO because violation of taste symmetry is required. At that order, they induce mixing of the operators, summarized in the quantities $\tilde{T}^{(n)}$, Eqs. (84) through (88), and $\tilde{Q}^{(n)}$, Eqs. (90) through (94). However, as long as all five $\mathcal{O}_n$ are analyzed simultaneously, there are no new low-energy constants induced by these effects: the constants β_n and β'_n are all already present in the continuum.

Effective operator mixings may come from three additional sources, weak-coupling perturbative corrections, corrections to the position-space spin-taste construction, and corrections to the taste identification of the operators and interpolating fields. I argue that any nonanalytic terms that arise from such mixings are effectively NNLO, higher order than what has been considered here.

Because the light staggered quark is converted to a naive quark in the lattice representatives of the operators, the relationship between the staggered and naive quark fields plays an important role in my analysis. In particular, a naive quark is equivalent to four copies of staggered quarks, and the resulting "copy symmetry" can be used to simplify the calculations. An interesting resulting feature is that the taste structure of the operators is not the same for all diagrams, but depends on the quark flow.

Lattice computations in Refs. [1,2] focused on the calculation of the quantity $\xi \equiv (f_{B_s}\sqrt{\hat{B}_{B_s}})/(f_{B_d}\sqrt{\hat{B}_{B_d}})$, which comes from the matrix element of operator $\mathcal{O}_1$. The chiral effects of the wrong spins were not known at the time of the HPQCD calculation [1] and were therefore omitted from the analysis and error estimate. In the Fermilab/MILC calculation [2], the complete rHMSχPT expressions were available, but the matrix elements of operators other than $\mathcal{O}_1$ were not calculated, preventing a direct inclusion of the wrong-spin effects. However, it was possible to estimate the error of omitting these effects by using a small subset of new data to investigate the other matrix elements. The result, $\xi = 1.268(63)$ included a 3.2% error from this effect, which was the second largest source of error. In the ongoing second-generation Fermilab/MILC project [40], matrix elements of all five operators $\mathcal{O}_n$ are being computed, which means that the complete rHMSχPT expressions can be used in the analysis, and there will be no "wrong-spin error." Of course, a chiral/continuum extrapolation error will remain.

For future lattice computations of mixing with "highly improved staggered quark" ensembles [41], taste violations are sufficiently reduced that the power counting used here, Eq. (81), may no longer be appropriate. Depending on the range of lattice spacings studied and the statistical errors in the data, taste violations may in fact be so small that continuum heavy meson χPT might prove adequate for describing the data. More likely, one will want to use the rHMSχPT forms calculated here, but it may be necessary in addition to include the NLO chiral effects of the operators that enter through weak-coupling perturbative mixing, since such effects may no longer be much smaller than taste-violating NLO effects. Including such effects in NLO rHMSχPT will however be straightforward, since the chiral logarithms for the complete set of operators, Eq. (1), have already been calculated above.

ACKNOWLEDGMENTS

I am indebted to J. Laiho, R. S. Van de Water, and C. Bouchard for help with various aspects of the calculation, and thank A. Kronfeld and all my other colleagues in the MILC and Fermilab/Lattice Collaborations for discussions. This work has been partially supported by the Department of Energy, under Grant No. DE-FG02-91ER40628. I also thank the Galileo Galilei Institute for Theoretical Physics for the hospitality and the INFN for partial support while this work was in progress.

APPENDIX: B PARAMETERS

It is sometimes convenient to express the mixing matrix elements in terms of B (or "bag") parameters. A fairly common set of definitions is given for example in Ref. [11]:

$$\langle \bar{B}_x^0 | O_1^x | B_x^0 \rangle = \frac{8}{3} M_{B_x}^2 f_{B_x}^2 B_{B_x}^{(1)}, \tag{A1}$$

$$\langle \bar{B}_x^0 | O_n^x | B_x^0 \rangle = \eta_n R^2 M_{B_x}^2 f_{B_x}^2 B_{B_x}^{(n)} \quad \text{for } n = 2, 3, 4, 5, \tag{A2}$$

where f_{B_x} is the decay constant of the B_x meson, M_{B_x} is its mass, $R \equiv M_{B_x}/(m_b + m_x)$, and $\eta_2 = -5/3$, $\eta_3 = 1/3$,

$\eta_4 = 2$, and $\eta_5 = 2/3$. Relativistic normalization of the states is assumed in these expressions.

The expression for the decay constant in rHMSχPT, including heavy-meson hyperfine and flavor splittings, is given in Eq. (6.20) of Ref. [7]. To convert it to the current notation, we just must replace the chiral logarithm functions J and ℓ with $\mathcal{H}$ and I using Eqs. (63) and (64). Using quantities defined above in Eqs. (62), (68), and (69), we may write the result as

$$f_{B_x}\sqrt{M_{B_x}} = \Phi_0\Big[1 + \frac{1}{2}(\mathcal{W}_{x\bar{b}} + \mathcal{T}^{(n)}_{x,\mathrm{Fig.3}} + \mathcal{T}^{(n)}_{x,\mathrm{Fig.4}})\Big]. \tag{A3}$$

It is not surprising that $\mathcal{W}_{x\bar{b}}$, $\mathcal{T}^{(n)}_{x,\mathrm{Fig.3}}$, and $\mathcal{T}^{(n)}_{x,\mathrm{Fig.4}}$ appear, because the wave function and the tadpole contributions of Figs. 3 and 4 are factorizable: they affect only one meson and one bilinear of the four-quark operators, so they are exactly the contributions that appear in the decay constant.

As always, heavy-light chiral perturbation theory is expressed in terms of the nonrelativistically normalized states of heavy quark effective theory. Thus the low-energy constant, Φ_0, that describes the decay constant at tree level in chiral perturbation theory includes a factor of $\sqrt{M_{B_x}}$. Similarly, with the relativistic normalization used Eqs. (A1) and (A2), one factor of M_{B_x} needs to be included in our expressions for these matrix elements in terms of the parameters β_n and β'_n. Taking these normalization factors into account, and using Eqs. (60), (61), and (A3), we have

$$B^{(1)}_{B_x} = \frac{\beta_1}{(8/3)\Phi_0^2}(1 + \mathcal{S}_x + \tilde{\mathcal{T}}^{(1)}_x + \mathcal{Q}^{(1)}_x + \tilde{\mathcal{Q}}^{(1)}_x) + \text{analytic terms} \tag{A4}$$

$$B^{(n)}_{B_x} = \frac{\beta_n}{\eta_n R^2 \Phi_0^2}(1 \pm \mathcal{S}_x + \tilde{\mathcal{T}}^{(n)}_x) + \frac{\beta'_n}{\eta_n R^2 \Phi_0^2}(\mathcal{Q}^{(n)}_x + \tilde{\mathcal{Q}}^{(n)}_x) + \text{analytic terms}, \tag{A5}$$

where $n = 2, \ldots, 5$ in the second equation, and the upper (plus) sign is for $n = 2$, 3, while the lower (minus) sign is for $n = 4$, 5. Here the wave function and tadpole contributions of Figs. 3 and 4 have canceled, and $\mathcal{S}_x$ is a new correct-spin tadpole term that comes only from the nonfactorizable tadpole diagrams, Figs. 5 and 6. Combining Eqs. (72) and (74) gives

$$\mathcal{S}_x = \frac{-i}{f_\pi^2}\Big\{\frac{1}{16}\sum_\rho N_\rho I_{X,\rho} + \frac{1}{3}\Big[R^{[2,2]}_{X_I}(\{M^{(2)}_{X_I}\};\{\mu_I\})\frac{\partial I_{X,I}}{\partial m^2_{X_I}} - \sum_{j\in\{M^{(2)}_I\}} D^{[2,2]}_{j,X_I}(\{M^{(2)}_{X_I}\};\{\mu_I\}) I_{j,I}\Big]\Big\}. \tag{A6}$$

The other chiral logarithm functions in Eqs. (A4) and (A5) are given in Eqs. (84) through (94). The analytic terms in Eqs. (A4) and (A5) have the same form as in Eq. (95) (with, of course, redefined low-energy constants).

[1] E. Gamiz *et al.* (HPQCD Collaboration), Phys. Rev. D **80**, 014503 (2009).
[2] A. Bazavov, C. Bernard, C. M. Bouchard, C. DeTar, M. Di Pierro, A. X. El-Khadra, R. T. Evans, E. D. Freeland *et al.* (The Fermilab Lattice and MILC Collaborations), Phys. Rev. D **86**, 034503 (2012).
[3] G. P. Lepage and B. A. Thacker, Nucl. Phys. B, Proc. Suppl. **4**, 199 (1988); B. A. Thacker and G. P. Lepage, Phys. Rev. D **43**, 196 (1991).
[4] A. X. El-Khadra, A. S. Kronfeld, and P. B. Mackenzie, Phys. Rev. D **55**, 3933 (1997).
[5] C. Aubin and C. Bernard, Phys. Rev. D **73**, 014515 (2006).
[6] C. G. Boyd and B. Grinstein, Nucl. Phys. **B442**, 205 (1995).
[7] A. Bazavov, C. Bernard, C. M. Bouchard, C. DeTar, M. Di Pierro, A. X. El-Khadra, R. T. Evans, E. D. Freeland *et al.* (Fermilab Lattice and MILC Collaborations), Phys. Rev. D **85**, 114506 (2012).
[8] M. Wingate, J. Shigemitsu, C. T. H. Davies, G. P. Lepage, and H. D. Trottier, Phys. Rev. D **67**, 054505 (2003).
[9] F. Gliozzi, Nucl. Phys. **B204**, 419 (1982); A. Duncan, R. Roskies, and H. Vaidya, Phys. Lett. **114B**, 439 (1982); H. Kluberg-Stern, A. Morel, O. Napoly, and B. Petersson, Nucl. Phys. **B220**, 447 (1983).
[10] C. Aubin and C. Bernard, Phys. Rev. D **76**, 014002 (2007).
[11] W. Detmold and C. J. D. Lin, Phys. Rev. D **76**, 014501 (2007).
[12] F. Gabbiani, E. Gabrielli, A. Masiero, and L. Silvestrini, Nucl. Phys. **B477**, 321 (1996).
[13] C. M. Bouchard, Report No. FERMILAB-THESIS-2011-32.
[14] S. Prelovsek, Phys. Rev. D **73**, 014506 (2006).
[15] C. Bernard, M. Golterman, and Y. Shamir, Phys. Rev. D **73**, 114511 (2006).
[16] Y. Shamir, Phys. Rev. D **71**, 034509 (2005).
[17] C. Bernard, Phys. Rev. D **73**, 114503 (2006).
[18] Y. Shamir, Phys. Rev. D **75**, 054503 (2007).
[19] C. Bernard, M. Golterman, and Y. Shamir, Phys. Rev. D **77**, 074505 (2008).
[20] S. R. Sharpe, Proc. Sci., LAT2006 (2006) 022 [arXiv:hep-lat/0610094].
[21] A. S. Kronfeld, Proc. Sci., LAT2007 (2007) 016 [arXiv:0711.0699].
[22] M. Golterman, Proc. Sci., CONFINEMENT8 (2008) 014 [arXiv:0812.3110].

[23] A. Bazavov, D. Toussaint, C. Bernard, J. Laiho, C. DeTar, L. Levkova, M. B. Oktay, S. Gottlieb *et al.*, Rev. Mod. Phys. **82**, 1349 (2010).
[24] G. C. Donald, C. T. H. Davies, E. Follana, and A. S. Kronfeld, Phys. Rev. D **84**, 054504 (2011).
[25] C. Aubin and C. Bernard, Phys. Rev. D **68**, 034014 (2003).
[26] C. Aubin and C. Bernard, Phys. Rev. D **68**, 074011 (2003).
[27] S. R. Sharpe, Phys. Rev. D **46**, 3146 (1992).
[28] C. Bernard (MILC Collaboration), Proc. Sci., LATTICE2012 (2012) 201 [arXiv:1211.0237].
[29] L. Wolfenstein, Phys. Lett. **164B**, 170 (1985).
[30] N. H. Christ (RBC and UKQCD Collaboration), arXiv:1012.6034.
[31] W.-J. Lee and S. R. Sharpe, Phys. Rev. D **60**, 114503 (1999).
[32] S. R. Sharpe and R. S. Van de Water, Phys. Rev. D **71**, 114505 (2005).
[33] S. Sharpe and N. Shoresh, Phys. Rev. D **64**, 114510 (2001).
[34] B. Grinstein, E. E. Jenkins, A. V. Manohar, M. J. Savage, and M. B. Wise, Nucl. Phys. **B380**, 369 (1992).
[35] M. F. L. Golterman and J. Smit, Nucl. Phys. **B245**, 61 (1984).
[36] S. R. Sharpe, Nucl. Phys. B, Proc. Suppl. **34**, 403 (1994).
[37] G. P. Lepage, arXiv:1111.2955.
[38] R. T. Evans *et al.* (Fermilab Lattice and MILC Collaborations), Proc. Sci., LAT2009 (2009) 245 [arXiv:0911.5432].
[39] R. S. Van de Water and S. R. Sharpe, Phys. Rev. D **73**, 014003 (2006).
[40] E. D. Freeland, C. M. Bouchard, C. Bernard, A. X. El-Khadra, E. Gamiz, A. S. Kronfeld, J. Laiho, and R. S. Van de Water, Proc. Sci., LATTICE2012 (2012) 124 [arXiv:1212.5470].
[41] E. Follana *et al.* (HPQCD/UKQCD Collaboration), Phys. Rev. D **75**, 054502 (2007); A. Bazavov *et al.* (MILC Collaboration), Phys. Rev. D **82**, 074501 (2010); **87**, 054505 (2013).